TOWARDS A CELL BASED SCREEN FOR MEDIATORS OF CELL DENSITY SENSING

by

MATTHEW L. ROMINE

(Under the Direction of Haini Cai)

ABSTRACT

Density of a cell culture is an important signal that regulates growth, metabolism, structure and locomotion of cells. Importantly, the responses of cultured cells to density also reveal mechanisms that govern animal development and diseases in vivo. We generated and characterized a density-responsive reporter system in transgenic Drosophila S2 cells. The transgenes are strongly induced in a cell density-dependent and reporter-independent fashion. The rapid and reversible induction occurs at the level of mRNA accumulation. We show that multiple components within the transgene, including a metal response element from the metallothionein gene, contribute to the reporter induction. Similarly, the reporter induction correlates with changes in multiple cell density and growth regulatory pathways including hypoxia, apoptosis, cell cycle and cytoskeletal pathways. We also tested the contribution of conditions including cell-to-cell and cell-to ECM contact and found the former to play a role in reporter induction. We conclude that our S2 transgenic system provides a quantitative and efficient cell-based platform for genome-wide and chemical screens for regulators of cell density responsive pathways. INDEX WORDS: S2 Cells, Density Sensing, Screen platform

TOWARDS A CELL BASED SCREEN FOR MEDIATORS OF CELL DENSITY SENSING AND CONTACT INHIBITION

by

MATTHEW L. ROMINE

B.S., University of Georgia, 2014

A Thesis Submitted to the Graduate Faculty of The University of Georgia in Partial Fulfillment of the Requirements for the Degree

MASTER OF SCIENCE

ATHENS, GEORGIA

2018

TOWARDS A CELL BASED SCREEN FOR MEDIATORS OF CELL DENSITY SENSING AND CONTACT INHIBITION

by

MATTHEW L. ROMINE

Major Professor: Haini Cai

Committee: Edward Kipreos
Karl Lechtreck

Electronic Version Approved:

Suzanne Barbour
Dean of the Graduate School
The University of Georgia
December 2018

TABLE OF CONTENTS

Page

LIST OF TABLES

Page

LIST OF FIGURES

Page

CHAPTER 1

INTRODUCTION AND LITERATURE REVIEW

1.1 Introduction:

The ability to detect changes in cell density is conserved from bacteria to mammalian cells. It allows for cells to modulate their behavior and division rate based on the available resources such as space and nutrients. A change in cell behavior based on cell density has been demonstrated by many experiments over the years. One of the earliest ones in 1954 showed that plating chicken heart fibroblasts leads to migration of the cells away from one another – this is where the term contact inhibition of locomotion was developed [1]. Another pioneering experiment was later done by making a streak in a confluent cell culture dish which lead to growth and division of the remaining cells into the newly cleared space [2]. These experiments and many others have linked cell density to many aspects of biology such as development, wound healing, and, when misregulated, cancer. Despite the significance of cell density in biology and disease much is still unknown about how it is detected and how it affects cell behavior. The remainder of this thesis seeks to explain current understandings of cell density responsive mechanisms and to investigate a possible transgenic cell culture system that could be used to elucidate some of the questions involved in cell density sensing and responsiveness.

1.2 S2 Cells:

The system developed is in the *Drosophila* S2 cell culture. These cells are a macrophage-like cells harvested from *Drosophila* embryos 20-24hrs old [3, 4]. They are accredited with being a very simple cell model with no cell polarity, no documented cadherin expression, no notch-delta expression, and having only a little integrin endogenously expressed [3, 5, 6]. S2 cells are useful tools for RNAi studies because they are able to phagocytose dsRNA naturally [6, 7]. Furthermore, they work well with fluorescence microscopy making them very useful for imaging studies [8, 9]. The cells can grow in room temperature and do not require any specific pH balances or atmospheric conditions which facilitate their use for experiments done in a typical lab environment [4, 8].

1.3 Hippo Pathway:

Core Machinery

In eukaryotes a well-known mediator for cell density signaling is the Hippo pathway. It has become associated with cell to cell contact, and its activity is dependent upon cell density. The pathway was originally discovered in *Drosophila* but has since been found in mammals, *C. elegans*, and yeast [10]. The core of the Hippo pathway involves the Hippo kinase (Mst1/2 in mammals) with its scaffold Salvador, Warts kinase (Lats1/2 in mammals) with its scaffold Mats, and finally the Yorkie (Yki) transcriptional coactivator (YAP/TAZ in mammals). Hereafter, the remaining description of the Hippo pathway will be in regards to *Drosophila*. There have been numerous studies which confirm that the loss of any of the Hippo pathway core components or hyperactivity of

Yki can lead to aberrant cell growth and tumor formation as well as developmental issues; and many of these studies are done through examining the cells' behavior as cells go from a sparse state to a dense state.

Yorkie is a transcriptional coactivator that does not directly bind to DNA but is seen to mainly compete with Tondu domain containing growth inhibitor (Tgi) with an interaction for a TEA-domain transcription factor called Scalloped (SD) [11, 12]. There are other transcription binding partners for Yki such as Homothorax and Smad, but these do not seem to account for Yki's activity in genetic studies, and therefore have taken a backseat to hippo pathway [13, 14]. When Yki and SD are paired, they promote the transcription of cell survival and antiapoptotic genes such as Cyclin E and DIAP1. However upon phosphorylation at Ser168 in the WW domain of Yorkie, it becomes sequestered in the cytoplasm, outside of the nucleus, by the 14-3-3 complex. The loss of Yki from the nucleus allows for Tgi to bind to SD and for the complex to assume a repressive role, inhibiting the transcription of Yki's pro-survival target genes such as Diap1 [12]. Yorkie's phosphorylation and inhibition is the end result of a kinase cascade. Generally, the Hippo kinase initiates the cascade once it is phosphorylated and activated by TAO-1 kinase or another Hippo kinase upon dimerization – this event is promoted by an increase in local concentration when Hippo is recruited to the membrane. The Hippo kinase begins by phosphorylating its scaffolding protein Salvador that helps protect Hippo from dephosphorylation by a protein phosphatase 2A (PP2A) called STRIPAK [15]. Then Hippo phosphorylates Mob, which is a coactivator and scaffold for Warts kinase. Phosphorylated Mob sequesters Warts, which can then be phosphorylated by Hippo kinase to become active. The activated Warts kinase then goes on to phosphorylate

Yorkie Ser168 leading to the transcription coactivator's inactivity. The Hippo pathway does exhibit a negative feedback regulatory mechanism as well. The Yki-SD active pair transcribes some members of the Hippo pathway such as Expanded, Merlin, Kibra; so when the Hippo pathway becomes active – causing Yki to be phosphorylated and then sequestered outside of the nucleus –, expression of its components diminishes.

Activation of the Hippo pathway

The activation of the Hippo pathway is seen as a multifaceted process because it is linked to many other signaling pathways. In fact many of the stresses a cell experiences during crowding such as a loss in cell attachment, an increase in cell-to-cell contacts, loss in cytoskeletal tension, loss in actin stress fibers, loss or change in cell polarity, a reduction of nutrients, and a change in secreted factors have all been found to affect the Hippo pathway [16, 17].

Adherent cells normally attach to the extracellular matrix (ECM) with focal adhesions (FAs), which consist of integrins, actin, and linker proteins such as vinculin and talin [18]. The cell and ECM then become engaged in an isometric tension, and the FAs serve as key mechanosensors for the cell to detect changes in the ECM. It has been found that cell spreading (mediated by FA's) provides the cell with high tension to the ECM and actin stress fibers. The tension and increased actin fibers promote Yki activity. Conversely loss of attachment to the ECM and subsequent loss of cytoskeletal tension leads to Hippo pathway activation and Yki inactivation [19-21].

Cell adhesion through cadherins has also been reported to regulate the Hippo pathway. It has been seen as a primary means of Hippo control in polarized cells [17, 19, 22]. E-cadherin has been found to inhibit the Hippo pathway in a tension-dependent

fashion [23, 24]. The cadherins are connected to the cytoskeleton, and when they experience tension, the force is transmitted to α-catenin. The tension stretches the α-catenin exposing a binding domain for the protein Jub, Ajuba in mammals. Jub bound to α-catenin sequesters Wrts inhibiting its activation. When the cadherin junction then loses tension, the α-catenin is no longer able to bind Jub which means that Wrts is now free to move towards Hippo and become activated.

Cell polarity is commonly looked at in the context of cell attachment. *Drosophila* has been a large source of studies because its epithelium is columnar and is dependent on polarity, and some of the *Drosophila* apical polarity proteins involved in Hippo signaling have also been found to have a conserved role in mammals [25-27]. Recently the apical Hippo components Crumbs, Merlin, Kibra, and Expanded have been found in separate domains [24]. Crumbs is an apico-junctional transmembrane protein that resides above adherins junctions in a region called the marginal zone, and it associates with Expanded [24, 28]. Wrts and Kibra typically co-localize to the medial-apical membrane. Both the Crumbs-Expanded and Merlin-Kibra complexes have been shown to mediate Hippo component clustering. The complexes group Hippo-Sav and Wrts-Mats kinases at the apical membrane, and this increase in concentration of the kinases results in increased activation of the complexes, which will result in Yki phosphorylation and inactivation [29, 30]. Furthermore Expanded and Merlin are FERM-domain proteins that connect the apical membrane to the cytoskeleton via spectrin providing a link between polarity and tension that has been demonstrated to affect Hippo pathway activation [29, 31]. If cytoskeletal tension is present, the apically located Hippo kinase complexes (sequestered there by Expanded and Merlin) are separated preventing Hippo dimerization and

activation; but when tension is lost, the apical-Hippo protein complexes are able to dimerize and become active.

Soluble factors have also been found to affect the Hippo pathway [10, 32]. Activation of certain G-protein coupled receptors (GPCRs) has been seen to affect the Hippo pathway [33, 34]. Shingosine-1-phosphate (S1P) and lysophosphatidic acid (LPA), both found in serum and documented to increase proliferation and migration, were found to inhibit Hippo pathway activation and reduce Yap phosphorylation – allowing for YAP to stay in the nucleus and continue aiding in transcription of pro-survival genes. This was dependent upon cytoskeletal integrity as S1P and LPA activated RhoA and loss of RhoA or disruption of the cytoskeleton resulted in Lats activation and Yap phosphorylation. In opposition to this, glucagon and epinephrine which affect different GPCRs activate the Hippo pathway and lead to Yap phosphorylation, and this is done by activation of protein kinase A (PKA). Activated PKA inhibits RhoA which results in Lats activation and Yap phosphorylation. The lack of nutrient factors has also been implicated in the Hippo pathway. AMP-activated protein kinase (AMPK) and mechanistic target of rampamycin (mTOR) are two pathways that respond to starvation and energy stress in a cell [35, 36]. In a mammalian cell study, AMPK was found to directly phosphorylate Yap preventing its ability to associate with the TEAD transcription factors [37]. In a fly study TOR inhibition was seen to inhibit Yki driven transcription via a nuclear exclusion mechanism where it was prevented from working while it was still localized to the nucleus [38].

1.3 Non-Hippo cell density response pathways:

<u>P53 mediated</u>

Along with the Hippo pathway, other cellular processes have been related to changes in cell density, and some also use the accompanying mechanical compression changes seen with an increase in cell density. Within the fly notum (epithelium on the thorax of *Drosophila* that grows sensory bristles), studies on cell delamination – process of cells detaching from epithelial layer – have shown that the combined cell compression and loss of apical area, brought on by high cell density in the limited space of the notum, lead to cell delamination and subsequent extrusion [39-44]. The cells that left the notum did so in two methods one being an apoptotic caspase mediated method and the other being a live cell extrusion once the apical area decreased, but for both it was found to be Hippo independent. This cell competition-elimination paradigm was also examined in mammalian kidney cells, and it focused on compressive forces from cell crowding causing p53 activation [45]. The p53 activation was a result of ROCK activation from compressive forces activating p38 which then activated p53, showing another means of crowding induced apoptosis.

Piezo 1

Piezo1 is a mechanically regulated Ca^{+2} ion channel [46]. It has been found to respond to tensile forces on the cytoskeleton [47]. The increase of tension activates Piezo1 increasing cellular Ca^{+2} levels and leading to cell mitosis via ERK activation [48]. The influx of calcium has also been tied to the Hippo pathway and cellular differentiation. With higher tensile forces, Piezo1 activation was seen to promote Yap activity as well, neuron formation, and inhibit Notch signaling to allow for enterocyte differentiation in the fly gut [47, 49]. Although Piezo1 responds to tension, which is associated with sparser cellular environments, Piezo localization can change to become

cytoplasmic, thereby limiting the ability for the cell to have a Ca^{+2} influx and mitotic promoting response when they become crowded [48]. This regulation of Piezo1 provides an interesting example of a mechanosensitive ion channel that responds to cell density changes.

TGFß

Transforming growth factor ß (TGFß) is a large family of signaling proteins secreted that has been found in many vertebrates and invertebrates including flies. [50, 51]. These signaling molecules serve to control cell proliferation, apoptosis, cell adhesion, differentiation, and more [50-52]. Their general mechanism of action occurs when the TGFß ligand binds to a heteromeric kinase receptor causing its dimerization, phosphorylation, and subsequent activation. Then the activated heteromeric receptor phosphorylates and activates the transcription factors SMAD to elicit the cellular response initiated by the ligand [53].

TGFß signaling has been implicated with cell density in a Hippo dependent manner whereby YAP/Taz (Yki) sequesters SMAD outside of the nucleus once the Hippo pathway is activated at high cell density [54]. However, another study done in cell culture has shown that increasing cell density can affect TGFß signaling independent of Hippo [52]. The authors found that a higher cell density can lead to the relocation of the TGFß receptors TßRI and TßRII to a basolateral location in polarized cells that is inaccessible to TGFß [52]. This localization was promoted by the presence of the cell to cell linkers E-cadherin, tight junctions and other Ca^{+2} linkers, and it was seen as means of maintaining epithelial integrity (essentially preventing an epithelial to mesenchymal transition (EMT)) at a high cell density when tissue formation is complete.

In addition to the cell-cell attachment mediated mechanism of TGFß regulation, cell-ECM attachment has also been found to regulate it. [55, 56]. TGFß is known to induce EMT and cell migration by increasing ECM components and reducing cell-cell junction linkers [53, 57]. Integrin activation can lead to an increase in TGFß signaling, but at higher cell densities, there is typically a reduction of integrins seen. This loss of integrins was found to lead to the loss of TGFß expression and signaling [56, 58]. These results demonstrate two different means whereby cell density regulates TGFß signaling, with the first being cell-cell regulated and the other being cell-ECM regulated.

Jak-STAT

Janus kinase (Jak) and the Signal transducers and activators of transcription (STAT) are proteins that interact and are commonly viewed together as the Jak-STAT pathway. Although it is highly simplified due to a lack of isoforms in *Drosophila*, this pathway is highly conserved between *Drosophila* and mammals [59, 60]. It involves the tyrosine kinase Jak that associates with transmembrane receptors that dimerize when bound to their extracellular ligand such as interferon, interleukin, and other growth factors in mammals or the Unpaired glycoproteins in *Drosophila* [61]. The dimerization of the receptor brings two Jak's in close proximity so that they can activate one another. Once activated JAK phosphorylates STAT causing STAT to dimerize. The dimerized STATs then translocate to the nucleus to activate transcription. The activation of the Jak-STAT pathway promotes many cellular behaviors such as cell division, cell death, migration, and more across many cell types including *Drosophila* S2 cells [62, 63]. This activation has been tied to other pathways, such as Notch-delta and even Hippo where these pathways regulate the expression of the Jak-STAT ligand [60, 64]. In relation to

cell density, a few studies have documented increased Jak-STAT activity when cell density increased, although the specific mechanism still remains unknown [65, 66]. Pathway activity has also been found to work to control cell numbers, insuring that there are not too many or too few cells in tissues such as the *Drosophila* ovary epithelium or the interfollicular stock [63, 67].

CHAPTER 2

A CELL DENSITY-RESPONSIVE REPORTER IN THE *DROSOPHILA* S2 CELLS

2.1 Abstract

Culture density is an important signal that regulates many aspects of cell properties and behaviors including metabolism, growth, cell structure, and locomotion. Importantly, the responses by cultured cells to density signals also uncover key mechanisms that govern animal development and diseases in vivo. We generated and characterized a density-responsive reporter system in transgenic *Drosophila* S2 cells. We show that the reporter genes are strongly induced in a cell density-dependent and reporter-independent fashion. The rapid and reversible induction occurs at the level of mRNA accumulation. We show that multiple DNA elements within the transgene sequences, including a metal response element from the *metallothionein* gene, contribute to the reporter induction. Similarly, the reporter induction correlates with changes in multiple cell density and growth regulatory pathways including hypoxia, apoptosis, cell cycle and cytoskeletal organization. The density-responsive reporter provides a sensitive and flexible cell-based platform for genome-wide and chemical screens for regulators of hypoxia and cell proliferation responses.

2.2 Introduction

Cell density sensing and growth regulation are among the most important cellular functions. Signals from developmental programs and cellular environment such as nutrient, oxygen and toxin levels, as well as cell-cell, cell-substrate interactions are

integrated to control multiple cellular apparatus that regulate the cell cycle, cell fate differentiation, cell migration, cytoskeletal structures, cell senescence and apoptosis [68-73]. These mechanisms ensure proper proliferation, differentiation, and organogenesis during animal development. Disruption of these functions could alter cell fates and lead to diseases. One of the most important mechanisms that regulate cell proliferation is contact inhibition [69, 74, 75]. It is known that cell-cell contacts in a crowded culture of normal cells lead to suppression of further cell proliferation, resulting in a confluent cell monolayer. In many cancer cells, such "contact inhibition" is abolished, leading in uncontrolled proliferation. This highlights the in vivo relevance of density sensing and responses as critical mechanisms that ensure normal tissue homeostasis. At the center of the highly conserved contact inhibition pathways are a series of phosphorylation events, mediated by the Hippo /Mst1/2 /Salvador and the Wts /LATs /Mats kinase complexes, which ultimately lead to the inhibition of the Yorkie/YAP/TAZ transcription factor and the down regulation of genes that promote cell proliferation and survival. Despite recent progress, the signaling and gene regulatory network that contribute to density sensing and growth control are not fully understood. We report here the development of a cell density reporter system in transgenic *Drosophila* cells [76]. The CaSpeR transposon-based transgene contains the green or red fluorescent protein (GFP or RFP), or other reporter genes [76-84]). In both transiently and stably transfected *Drosophila* cells, these reporters respond strongly to changing cell density. We showed that the rapid and reversible induction occurs at the level of mRNA accumulation and is mediated by multiple components in the transgene. We present evidence that a small portion of the responses at the mRNA level is mediated by pericellular hypoxia via a *metallothionein*

(MT) enhancer in the transgene. However, additional density-dependent signals other than hypoxia are responsible for the strong GFP or RFP induction. The reporter activation correlates with changes in markers of several cellular pathways that respond to cell density. These include markers of cell cycle regulation and apoptosis, the Hippo pathway, a hypoxia marker, and factors involved in cytoskeleton and motility. Taken together, the density-responsive reporter could be customized in its *cis and trans* components to provide quantitative and efficient platforms for drug/chemical or RNAi screens for regulators of cell density response and cell growth and proliferation.

2.3 Results

Induction of reporter genes by high cell density in transiently transfected *Drosophila* S2 cells

We have recently discovered that the GFP expression in CA-MT-eve-GFP (MG) transiently transfected S2 cells to be strongly induced at high cell density (Figure 2.1A-E). At $5x10^5$/mL, the total GFP level, as defined by Fluorescent Activated Cell Sorting (FACS) assays, is low (Figure 2.1B-C, 2.1H. see methods). When the culture density increases to 1.4-1.8 $x10^7$/mL, the GFP level rises by over 30-fold, both from an increase in the mean GFP level and the frequency of GFP-positive cells. This occurs as these freshly transfected cells divide and presumably as the copy number of the transgene reduces (Figure 2.1F-H). In comparison, GFP induction by 1 mM Cu^{2+} is only 5-7 fold (Figure 2.1H). Next we tested whether the density response is GFP-specific. In S2 cells transfected with CA-MT-eve-RFP (MR, Figure 2.2A-F) and CA-MT-eve-LacZ (MZ, Figure 2.2G-H) constructs, the reporters are also strongly induced by high cell density

[77, 81]. Activation of the MG transgene reporter by high cell density is also observed in transiently transfected *Drosophila* Kc cells, although the fold of induction is lower than that seen in S2 cells, possibly due relative higher basal GFP level in low-density cells (Figure 2.2I).

Reporter gene activation occurs mainly through mRNA accumulation

Gene regulation can occur at many different levels including rate of transcription, mRNA degradation, as well as protein synthesis, modification, maturation, and degradation. The fact that the β-galactosidase enzyme is induced at high cell density suggests that the induction mechanism is not specific to the property and function of fluorescent proteins. In order to distinguish whether the reporter gene activation occurs at mRNA or protein level, we performed reverse transcriptase-mediated PCR (RT-PCR) to assess the reporter mRNA level in low- and high-density cell cultures, respectively. As seen in (Figure 2.3), quantitation by RT-PCR followed by gel electrophoresis suggests a ~30-40x increase in the GFP mRNA level under high cell density over low density. This is comparable to the level of reporter activation as quantitated by FACS (Figure 2.2). This result suggests that the GFP increase occurs mostly at the level of mRNA accumulation. A similar result is also seen with the RFP reporter (see below).

Establishing stably transfected cell lines that exhibit density-responsive reporter activation

The density responsive reporter induction is potentially useful for biochemical studies and for developing large-scale cell-based screens for regulators of cell density-related processes. As such it is imperative to establish and characterize stably integrated

transgenic cell lines that provide consistent cell sources and display well calibrated reporter activation behaviors. P-element-based transposition has been shown to produce predominantly low copy number solitary insertions in stably transfected *Drosophila* cells [85]. We have also reported the use of the *Drosophila* P element transposon for improving efficiency of genomic integration and single copy transgene insertion in the S2 cells [76]. As a first step towards generating stable reporter lines that respond to cell density, we co-transfected S2 cells with the MG or MR transgenes and pTurbo, a plasmid encoding the P element transposase (Figure 2.4), [76, 86]). The GFP or RFP positive cells were enriched by consecutive FACS sorting over the course of eight months to reach stable polyclonal GFP or RFP cell populations that display a broad reporter expression range at low culture density (Figure 2.4A, E). We observed a lower mean reporter expression in these cells than in the transiently transfected cells, due to a reduction in the transgene copy number. Quantitation of transgene DNA by qPCR indicates that the polyclonal MR cells contain an average of 10 copies of transgene per cell. Under high cell density, an average of 3-fold increase in the mean fluorescence level is observed in both MG and MR population, with large variations in the behavior of individual cell clones (Figure 2.4B, F). In the MG population, the percentage of positively gated cells increases from 17% to 83%, a ~5x increase, resulting in a ~15x increase in the total GFP as quantitated by FACS and qRT-PCR (Figure 2.4C-D). The MR population, due to its higher purity, showed a more moderate increase in the RFP level since there is a less significant change in the number of fluorescent cells, as quantitated by both FACS and by qRT-PCR (Figure 2.4G-H). In summary, both MG and MR transgenes exhibit strong reporter induction by high cell density as integrated copies in the genome and

chromosomal environment. These stable transgenic populations are further characterized below to understand the density-mediated induction of reporters.

Reporter induction is density dependable and reversible

We used the stable MG or MR cells to first examining the dynamics of the reporter induction during cell growth. We found that the GFP or RFP levels begin to rise even at low-intermediate concentration (1-2 x10^6/mL), when cells are still actively proliferating (Figure 2.5A-C, E-G, I). They continue to increase exponentially with cell density up to peak levels at ~1.6x10^7/mL (Figure 2.5A-C, E-G, I). Similarly, the GFP mRNA exhibited a similar exponential increase according to the cell density (Figure 2.5J). Importantly, the GFP and RFP induction is reversible when cell density is reduced to 5x10^5/mL through subculture and is maintained at this level (Figure 2.5D, H, K). The GFP mRNA decreases rapidly, reaching the basal level within 48 hours (Figure 2.5L). The GFP protein decays more slowly, reducing to basal level in 3-4 days (Figure 2.5J). This could be due to the perdurance of the fluorescent proteins. These observations are also consistent with the finding that the density-mediated induction occurs mainly at the transcript level.

Analysis of transgenes for DNA sequences that mediate reporter activation at high density

As a first step towards identifying the *cis* and *trans* components that mediate reporter activation at high cell density, we dissected the transgene DNA elements in reporter induction assays. Besides the reporter coding regions, the transgene plasmid

contains three major functional elements: the MT enhancer, the *eve* basal promoter and the CaSpeR vector (Figure 2.6A). The MT enhancer from the *Drosophila metallothionine* gene interacts with the metal responding factor MTF-1 to drive strong transcriptional activation of either homologous and heterologous genes both in vivo and in cultured cells [78, 87]. The *eve* basal promoter contains a 42-bp upstream sequence and a canonical TATA box. It exhibits low basal activity but mediates robust activation when combined with a variety of enhancers in cultured cells and transgenic *Drosophila* [79, 80, 88]. The Casper vector contains *Drosophila* transposon P-elements. We have modified the original vector to remove the adult fly selection marker gene *miniwhite* [76, 89-91]. The enhancer and promoter pairing was combined with a GFP reporter in selected vector backbones and introduced into *Drosophila* S2 cells via transient transfection. We first tested the role of the MT enhancer in either Cu^{++} or high density-mediated GFP induction (Figure 2.6B-D). Deletion of the MT enhancer resulted in a dramatic loss in the GFP induction by either Cu^{++} or by high cell density, although the fold of induction by cell density remains high due to a comparable drop in the basal level (Figure 2.6). Replacing MT with 2PE, a mesoderm enhancer from the *twist* gene, which is known to be active in the S2 cells, restores the reporter induction by high cell density but not by Cu^{++} [92-94]. This result indicates that the cell density response is not dependent on the MT enhancer, which is known to mediate signals in multiple responses including heavy metal detoxification and hypoxia responses [87, 95, 96]. Rather, the MT and 2PE enhancers may serve to augment the density response.

We next replaced the *eve* basal promoter with the *Alcohol dehydrogenase (Adh)* or *Heatshock protein 70 (Hsp70)* promoter. The *Adh* and the *Hsp70* basal promoters

have been used widely to drive gene expression in both transgenic *Drosophila* and S2 cells [81, 97]. Swapping the *eve* promoter with the *Adh* promoter causes a substantial loss in the magnitude of density-mediated induction but an increase in the relative fold of induction due to a reduced basal transcription level. In contrast, the response to Cu^{++} decreased both in magnitude and in fold of induction (Figure 2.6B-C). Replacing the *eve* basal promoter by the *Hsp70* promoter lead to a stronger loss both in Cu^{++} and density-mediated induction. Taken together, although the *Adh* promoter appears to be the most specific and sensitive in responding to cell density cues, the *eve* promoter provides the most robust response and more suited for diverse applications.

We further evaluated the contribution of the transgene vector by switching out the CaSpeR vector with the pTOPO vector (Invitrogen). This dramatically reduced GFP responses to both density and metal inducing cues, although the fold of induction remains comparable to CaSpeR-based combinations (Figure 2.6B-D). This result suggests that sequences within the CaSpeR vector may mediate signals from high cell density. Taken together, our DNA dissection analysis indicates that multiple elements in the original MG transgene collaborate to maximize the reporter response to high cell density. Although none of the elements is essential for the density response, the CA-MT-eve combination appears to optimize the reporter induction by high cell density possibly in a synergistic fashion.

Reporter mRNA induction is contributed in part by hypoxia through the MT enhancer

The role of the MT enhancer in density-driven reporter activation is intriguing. It has been reported that oxygen partial pressure in the pericellular space can be strongly

affected by cell density and media height [98-101]. As a result, extreme hypoxia condition may exist in pericellular space under high cell density. Importantly, hypoxia has been shown to activate the *metallothionein* gene through the cooperative binding of MTF-1 and HF-1 factors on the MT enhancer [96, 102]. To clarify the roles of hypoxia in reporter response to cell density, we compared the mRNA induction of the florescent reporters with an *in vivo* hypoxia marker *lactose dehydrogenase (LDH)* under various hypoxic conditions (Figure 2.7). We first tested the MT-RFP transgene induction using the hypoxia-mimicking drug Deferoxamine Mesylate (DFO, Figure 2.8). After a 24-hour treatment of 50, 100, or 200μM DFO, concentrations known to induce hypoxia in cultured cells, we observed approximately a 3-fold increase in the *LDH* mRNA [103-105]. The same conditions did not significantly alter the RFP mRNA level (Figure 2.8). Next we tested the effect of low oxygen partial pressure using a hypoxia incubator chamber (Stemcell Technologies). After a 24-hour treatment under 4% or 1% O_2 partial pressure, the *LDH* mRNA level increased by 200 and 125-fold, respectively (Figure 2.7A-B). The same conditions also induced the GFP mRNA by 9 and 7-fold, respectively. Deletion of the MT enhancer (ΔMT, Figure 2.7D) or replacing it with the 2PE enhancer (2PE, Figure 2.7E) greatly diminished the GFP response to hypoxia, resulting in a 2.3-fold and 1.5-fold increase of GFP mRNA under 1% O_2, respectively. In comparison, 1% O_2 activated the *LDH* mRNA by over 60-fold in both ΔMT and 2PE transgenes (Figure 2.7D-E). These results suggest that the reporter mRNA can be induced by hypoxia at the mRNA level, and this effect is largely mediated through the MT enhancer.

Next we compared the induction of LDH and GFP by high density with those by hypoxia (Figure 2.7B). Under high cell density (1.6x10^7/mL), there is a 5x increase in the LDH mRNA expression, indicating that the cells are mildly hypoxic under high density. However, reporter mRNA level increased by 31-fold, suggesting that this increase is unlikely to be mainly due to hypoxia (2.7B). This conclusion is further supported by the robust reporter mRNA induction at high density in the ΔMT and 2PE cells, in which the GFP no longer respond to hypoxia but still respond to crowding (Figure 2.7D-E).

Hypoxia has been known to suppress protein translation [106-109]. This suppression could potentially affect the reporter read out at high cell density where pericellular hypoxia occurs. To examine whether the mild induction by hypoxia at the mRNA level is reflected in reporter fluorescence, we conducted FACS analysis the MG-containing cells under 1% oxygen partial pressure. We found no significant change in the fluorescence level under hypoxia (Figure 2.7C). Taken together, our results indicate that although hypoxia-related signals affect reporter mRNA expression at high cell density, this effect does not affect the reporter fluorescence level, and can be can be minimized by the removal of the MT enhancer.

Density correlative changes in selected genes and pathways

Besides hypoxia, many signaling pathways are involved in density sensing and growth control. To begin identifying the signals that activate our reporter expression, we surveyed the concurrent changes in several reporter-related cellular genes and transcription targets of growth-related pathways. As the reporter induction occurs strongly and more consistently between rapid proliferating density (4x10^6/mL) and

post-cycling confluence density (1.6x10^7/mL), we quantitated the mRNA level of the candidate genes at these two cell densities. We first compared the reporter induction to *metallothionein* (*MTA)* and *MTF-1*, the transcription factor that binds to the MT enhancers and activates *MTA* [83, 84]. We found that both *MTA* and *MTF-1* mRNAs increased at high cell density, although the changes in their mRNA level appear to be less dramatic than GFP (Figure 2.9A). This result is not surprising as similar density-dependent activations of *MTA* were reported in HeLa and lymphoma cells, although the changes are more moderate [95]. In addition, *MTA* is also activated by hypoxia via its metal response element [110]. Our results indicate that the transgene reporter is induced in parallel with the *metallothionein* gene by increasing cell density, likely through the MT enhancer and contributed by hypoxia. However, since significant level of reporter activation remains in the absence of the MT enhancer (Figure 2.6C-D), additional *cis*- and *trans*- signals may also be involved in reporter induction.

Next we examined the changes in *Cyclin E (CycE)*, the cyclin that promotes G1-S transition and is overexpressed in many cancer cells [111, 112]. We found that the *CycE* mRNA level reduces as cells enter quiescence at high density. In contrast, the level of *Drosophila* proapoptotic gene *reaper (rpr),* a FasC death factor receptor homolog, was elevated at high cell density [113-115]. The changes in both *CycE* and *rpr* are consistent with their role in growth regulation, although the magnitude of their change is much lower than that seen with the GFP reporter. We also examined *Expanded (Ex)* and *Kibra*, two proteins involved in the contact inhibition of cell proliferation. *Ex* and *Kibra* signal to the Hippo pathway, leading to the inactivation of *Yorkie (Yki)* and the down regulation

of growth and proliferation [27, 116-118]. Both *Ex* and *Kibra* genes are also targets of *Yorkie* activation and therefore are expected to down-regulate at high cell density. This is indeed what we observed – both *Ex* and *Kibra* mRNA showed significant reduction at high cell density (Figure 2.9C). Another important pathway related to cell density and proliferation is the cytoskeletal organization. Cancer cells have different cytoskeleton organization [119, 120]. Mechanical forces in tissue and cellular environment have been known to act through integrin and actin network to regulate growth [121-123]. The alpha-smooth-muscle Actin (α-SMA) and the stress fibers it forms can regulate the Hippo pathway by promoting Yki/YAP nuclear translocation in mammals [27, 124-126]. Cytoplasmic beta- and gamma-actin are also known to be down-regulated at high cell density in mouse fibroblasts, often concomitant with F-actin depolymerization [127]. We observed a reduction in the mRNA level of *Actin 88F*, the *Drosophila* alpha-SMA, at high cell density (Figure 2.9D). We further examined the mRNA level of *gelsolin,* an actin-binding protein that controls the actin filament assembly and disassembly [128-131]. We found it to be also reduced at high cell density. Down-regulation of gelsolin contributes to the disorganized cytoskeleton present in many cancer cells. Our results suggest the both the amount and the organization of the actin network are decreased when S2 cells reach post-confluence density. Taken together, we have examined changes in several cellular pathways related to cell density and growth regulation, hoping to identify transcriptional targets that correlate with the reporter induction both in timing and amplitude. Among the genes we tested, the *MTA* mRNA level responds to cell density in a parallel fashion as the GFP reporter. In comparison, markers of cell cycle regulation,

apoptosis, contact inhibition and cytoskeletal organization showed significant but less dramatic changes.

2.4 Discussion

We have characterized a novel reporter system that responds to cell density in transient and stably transformed *Drosophila* S2 cells. We showed that the transgenic reporters are induced in a culture density-dependent and reporter-independent fashion. The rapid and reversible induction of the GFP or RFP transgene is reflected both in the mRNA level and in the mean fluorescence of the cells. These results suggest a quantitative signal(s) that correlates with cell density and argue against a threshold or all-or-none response. Our results indicate that multiple components within the transgene DNA respond to the density-dependent signals to possibly synergistically induce the reporter expression. Among the elements we tested, the MT enhancer appears to mediate metal response, hypoxia response and high cell density response. Replacing MT with the 2PE enhancer can eliminate the responses from the metal and hypoxia but not density-mediated reporter activation, suggesting that distinct signals contribute to reporter induction via these DNA sequences. We further show that the *eve* promoter and the CaSpeR vector sequences in the transgene also help to optimize the density-induced reporter activation. We found that several growth-related pathways are regulated in accordance with the reporter induction as cell density increases, including components of the pathways involved in cell cycle regulation, apoptosis, contact inhibition and cytoskeleton organization. However, further work is needed to identify the specific signal(s) that directly trigger the reporter induction. Taken together, our analysis suggests that multiple *cis*- and *trans*- factors intercept with cell density and growth regulation signals. These results support the potential of the sensitive and versatile

density response in developing a cell-based screening platform for genome-wide RNAi knockdown and/or chemical screens for regulators of cell proliferation responses.

The role of the MT enhancer in cell crowding and hypoxia

The *metallothionein (MT)* genes encode small cysteine-rich proteins that chelate divalent metal ions like Zn^{++}, Cu^{++} and Cd^{++} [132-134]. They are found widely in eukaryotic species, often in multiple copies and expressed constitutively in most tissues and organs. They are involved in metal metabolism and detoxification, reactive oxygen species scavenging, stress response and neuronal growth regulation [135, 136]. Besides responding to metals, certain isoforms of mammalian MT's (MT-1 and 2) are induced by glucocorticoids while others, such as MT-3, inhibit neurite outgrowth and neuronal survival, and are deficient in patients with Alzheimer's disease [136]. Therefore, the MT genes are likely to respond to diverse signaling inputs and perform distinct function in different tissues. The MT enhancer we used in this study is isolated from the regulatory region of the *Drosophila* MT-A gene [76, 78]. MT-A does not direct correspond to a specific mammalian ortholog but it shares the basic structure and function characteristics of the MT proteins. Previous studies indicate that MT-A could be induced by several signaling pathways through its enhancer/promoter sequences. Our finding that the MT enhancer responds to Cu^{++}, hypoxia, and density-induced signals are also consistent with the previous observations. Further fragmentation or internal deletions may reveal sequences that specifically respond to signal from high cell density.

Hypoxia response is an important mechanism that can drastically alter cell physiology and gene expression profiles. It also affects cell fate decisions including growth and differentiation [137-140]. Our MG reporter responds to low oxygen partial pressure less dramatically than LDH, an *in vivo* hypoxia marker (Figure 2.7B-C). But it responds to high cell density more dramatically than LDH, suggesting that although pericellular hypoxia exists under high cell density, it plays a minor role in reporter induction that other density-related signal [98-101]. This is consistent with the observation that the ΔMT transgene, which no longer respond to hypoxia, still respond to high cell density. Importantly, hypoxia is known to suppress protein translation [106-109]. Under severe hypoxia (1% P_{O2}) bulk protein synthesis could reduce by over 75% in just two hours [106]. This down regulation is known to be independent of PI3/Akt and HIF-1α, but mediated through the repression of mTOR, which acts as an oxygen sensor [141, 142]. Consistent with these findings, we observed no increase in the florescent protein level after hypoxia despite increases in the mRNA level. This suppression of translation can be alleviated by RNAi knockdown of elF2B-Δ and Tsc-2, two proteins responsible for inhibiting translation under hypoxia, is know to rescue GFP protein expression under hypoxia [106]. In summary, the transgene platform, with its strong readout and versatile cis and trans modules, provides a good basis for developing targeted screening strategies.

Developing a cell-based screening platform for regulators of cell density signaling

Cell culture system provides powerful advantages that complement *in vivo* studies. The homogeneity of the cell populations allows consistent and uniform response, thus permitting sensitive and quantitative assessment both in biochemical and cell biological behaviors. The cell-based assays are amenable to chemical and molecular genetic

treatment such as drug and small chemical screens or genome-wide RNAi or CRISPR-based screens for identifying genes and pathways regulating a variety of cellular function [143-147]. Our cell density reporter can be adapted for assays and screens on cell growth and behaviors, including signaling and gene regulation targets during cell cycle progression, apoptosis, contact inhibition of proliferation and cell migration, as well as cytoskeletal organization. The system could be customization at the level of transgene DNA composition, which allows selective response to cell-density and/or hypoxia differentially. Combination of reporter lines containing different transgenes allows multiplex screening for different density-responsive targets. RNAi knock down of elF2B-Δ and Tsc-2 may allow use in hypoxia -related screen. Additional reporters, such as luciferase, could be used for more quantitative readout. Although we have only tested reporter response to cell density in two *Drosophila* cell lines, addition cell types and species may be compatible with the reporter system. Our reporter can integrate into the genome both via the classic non-homologous insertion of long tandem arrays or through transposase-mediated single copy insertion in different cell clones [148, 149]. As a result, these clones may response with different intensity and timing to various signaling events and could may be exploited in screens.

2.5 Materials and Methods

S2 cell culture and transfection

Drosophila Schneider's Line 2 (S2) cells were maintained in HyQ SFX-Insect serum-free medium (HyClone) at 25°C. Cells were sub-cultured every 6 days. The DNAs used for transfection were prepared using the Qiagen Plasmid Mini Kit. For transfection S2 cells were sub-cultured 3-5 days before transfection, $5x10^5$ cells in 1 ml medium were

aliquoted into each well of a 12-well plate. After cells had attached to the bottom of the well, they were gently washed once with 1 ml of fresh medium and soaked in 0.5 ml of transfection cocktail (1 μg of assay construct and 2.5 μl of Cellfectin reagent in 0.5 ml medium). For stable transfection, pTurbo plasmid containing the P-element transposase was mixed with the assay construction at a ratio of 1 to 10. The transfection cocktail was replaced with fresh medium after 5 hour of incubation. Cells were normally induced with 1 mM $CuSO_4$ 24 hours after transfection. For polyclonal stably transfected cells, transgenic cells were passaged continuously for 6-8 weeks before FACS sorting enrichment and continued until population reach >97% transgenic.

Construction of DNA plasmids used in S2 cell reporter expression

The pCA-MT-eb-GFP (MG) and pCA-MT-eb-RFP (MR) plasmids was described previously [76, 77]. The pCA-MT-eb-lacZ (MZ) plasmid was constructed by removing the miniwhite reporter in the *Drosophila* germline transformation vector pCaSpeR-eb-lacZ plasmid by Nsi I and Eco RI digestion and replacing it with the Metallothionein (MT) enhancer [79, 150]. To generate the pCA-Delta-GFP plasmid, the MT element was removed through an EcoRI digestion and the resulting vector religated. To generate the pCA-2PE-GFP plasmid, the MG plasmid was digested with Bam H1 to remove the MT-*eve* promoter, and ligated to a Bam HI fragment containing 2PE-*eve* promoter fragment. For Adh and Hsp70 promoter swap plasmids, the 1.6-kb *Hsp70* promoter and the 1.4-kb *Adh* promoter was PCR cloned and excited out from the pTOPO vector as an EcoR I-BamH I fragment and ligated MT and GFP region (see Table 1 for PCR primers). For pTOPO based constructs, the MT/Delta/2PE-eb-GFP region was removed from MG using HindIII and PstI sites.

Reporter induction and quantitation

For Cu^{++} induction, CuSO4 is added to the cell media to a final concentration of 1 mM 24 hours prior to FACS analysis or mRNA preparation for qRT-PCR analysis. For crowding induction, cells were cultured for 5-8 days to reach $1.6x10^7$/mL prior to FACS analysis or mRNA preparation for qRT-PCR analysis. Fluorescence microscopy and flow cytometry analysis were done 24 hours after induction. Cell images were taken with a digital camera attached to a Zeiss Axioplan 2 fluorescence microscope. FACS was performed using a FACSCalibur flow cytometer (Becton Dickinson Immunocytometry Systems) on $2.5\text{-}5x10^4$ cells each sample. For each sample, two biological replicates were performed. Data analysis was done using the FlowJo software. The fold of induction is calculated as $(\text{frequency x mean fluorescence})_{\text{uninduced}}/(\text{frequency x mean fluorescence})_{\text{induced}}$. For all bargraphs, the error is calculated as: SEM = standard deviation (SD)/square root [replicate number (N)]. The LacZ reporter activity was quantitated using the Invitrogen β-Gal Assay Kit (Catalog no. K1455-01) following the protocol therein.

Reporter induction and quantitation

For Cu^{++} induction, CuSO4 is added to the cell media to a final concentration of 1 mM 24 hours prior to FACS analysis or mRNA preparation for qRT-PCR analysis. For crowding induction, cells were cultured for 5-8 days to reach $1.6x10^7$/mL prior to FACS analysis or mRNA preparation for qRT-PCR analysis. Fluorescence microscopy and flow cytometry analysis were done 24 hours after induction. Cell images were taken with a digital camera attached to a Zeiss Axioplan 2 fluorescence microscope. FACS was performed using a FACSCalibur flow cytometer (Becton Dickinson Immunocytometry Systems) on $2.5\text{-}5x10^4$ cells each sample. For each sample, two biological replicates were performed.

Data analysis was done using the FlowJo software. The fold of induction is calculated as (frequency x mean fluorescence)$_{uninduced}$/(frequency x mean fluorescence)$_{induced}$. For all bargraphs, the error is calculated as: SEM = standard deviation (SD)/square root [replicate number (N)]. The LacZ reporter activity was quantitated using the Invitrogen β-Gal Assay Kit (Catalog no. K1455-01) following the protocol therein.

RNA preparation, cDNA preparation, RT-PCR and qRT-PCR

For mRNA analysis in Figure 2, the total RNA was prepared using the TRIzol reagent (Invitrogen Catalog no. 15569018) following the protocol therein. Multiplex RT-PCR reactions using gene-specific primers (see Table 1 see primer sequences) was performed using isolated RNAs as templates. Gel electrophoresis was performed on a 2% agarose gel and the specific bands of the product was quantitated using a BioRad gel imager. For the rest of the manuscript, mRNA quantitation was performed using qRT-PCR. Briefly, cDNA library was generated using oligo-d(T) primer and the Superscript III reverse transcriptase Kit (Invitrogen). Quantitative PCR (qPCR) analysis was done to quantify gene expression using SYBR Green Supermix (Bio-Rad). For each sample, 2-3 biological replicates and two qPCR replicates were performed.

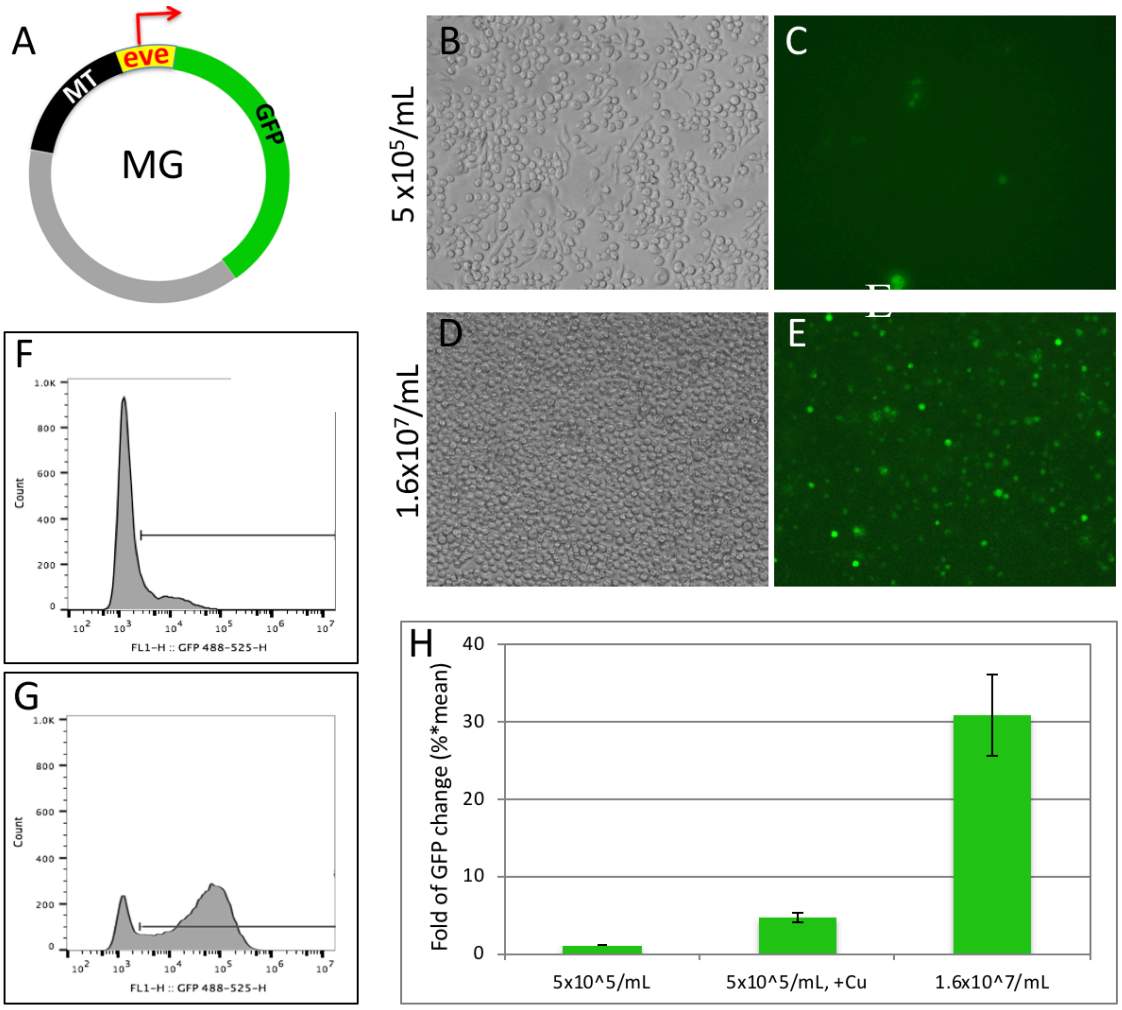
A
MT
eve
GFP
MG
B
C
5 x10^5/mL
D
E
1.6x10^7/mL
F
Count
FL1-H :: GFP 488-525-H
G
Count
FL1-H :: GFP 488-525-H
H
Fold of GFP change (%*mean)
40
30
20
10
0
5x10^5/mL
5x10^5/mL, +Cu
1.6x10^7/mL

Figure 2.1

Figure 2.1 GFP reporter is activated by cell crowding in *Drosophila* S2 cells

A.) Schematic of the MT-GFP (MG) transgene. Transgene components are shown in different colors: CaSpeR vector (grey), MT enhancer (black), *evenskipped* basal promoter (light yellow) and the GFP reporter gene (green). The red arrow: Transcription start site (+1). B-E.) Differential interference contract (DIC, left) and epifluorescence (right) microscopy images of MG-containing cells at low ($5x10^5$/mL, top) and high ($1.6x10^7$/mL, bottom) culture density. F-G.) Fluorescent Activated Cell Sorting (FACS) histogram of MG-containing cells at low ($5x10^5$/mL, F) and high ($1.6x10^7$/mL, **G**) culture density. X-axes: log scale of GFP level; Y-axis: cells number at indicated GFP level. Horizontal bar: GFP positive cells with fluorescence level above $2.5x10^3$. H. Bar graph quantitation of GFP induction by 1mM $CuSO_4$ and by high cell density. The total GFP fluorescence level is calculated as the percentage of the GFP positive cells multiplied by mean GFP intensity of these cells. Left, MG-containing cells at low density ($5x10^5$/mL) without $CuSO_4$. The GFP level in these cells is used as 1 to calculate fold of induction. Middle, MG-containing cells at low density incubated for 24 hours with 1mM $CuSO_4$. Right, MG-containing cells at high density ($1.6x10^7$/mL) in the absence of $CuSO_4$.

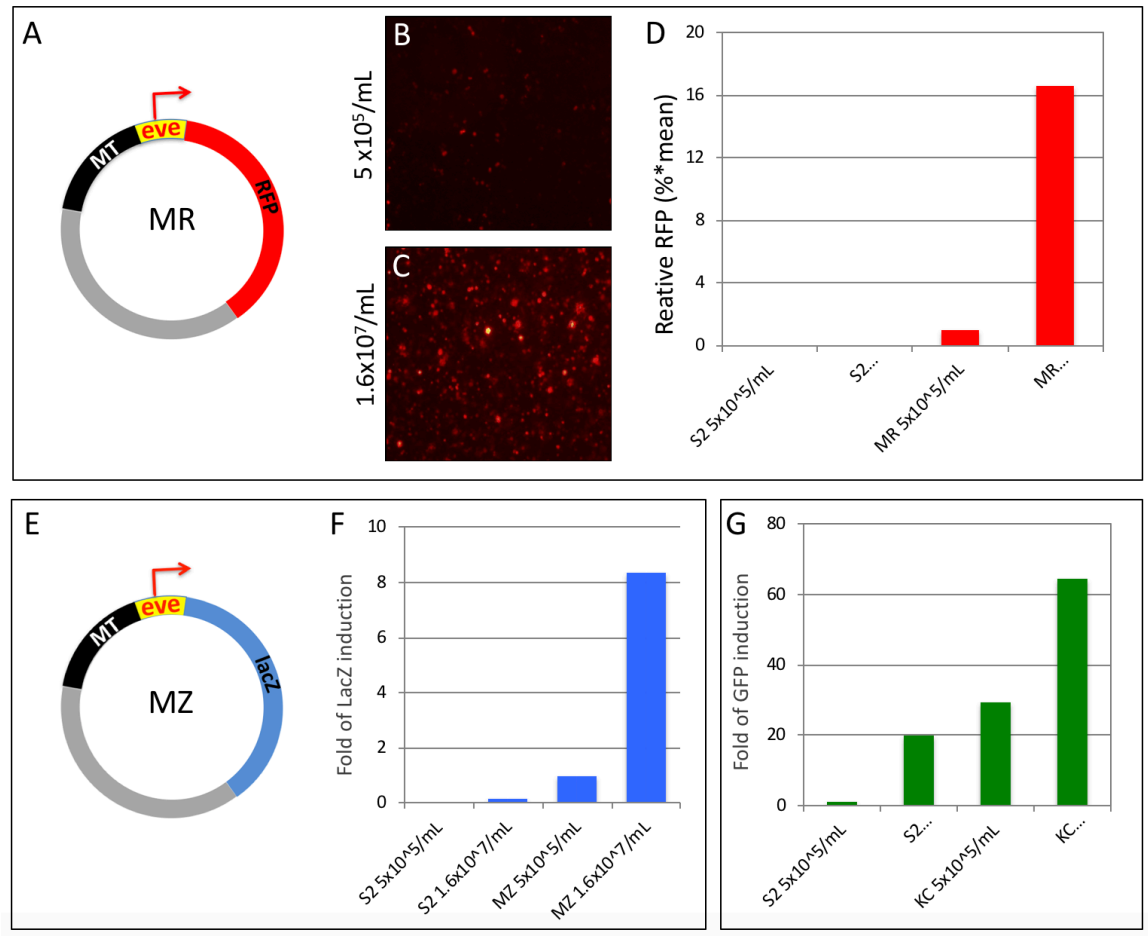
A
MT
eve
RFP
MR
B
5 x10^5/mL
C
1.6x10^7/mL
D
Reative RFP (%*mean)
20
16
12
8
4
0
S2 5x10^5/mL
S2...
MR 5x10^5/mL
MR...
E
MT
eve
lacZ
MZ
F
Fold of LacZ induction
10
8
6
4
2
0
S2 5x10^5/mL
S2 1.6x10^7/mL
MZ 5x10^5/mL
MZ 1.6x10^7/mL
G
Fold of GFP induction
80
60
40
20
0
S2 5x10^5/mL
S2...
KC 5x10^5/mL
KC...

Figure 2.2

Figure 2.2: Cell crowding induction of multiple reporters and in *Drosophila* Kc cells. A-D**)** RFP reporter induction by high cell density in S2 cells. A. Schematic of the MT-RFP (MR) transgene. Transgene components are shown as in Figure 1 except the RFP coding region is shown in red. B-C**)** Epifluorescent microscopy images of MR-containing cells at low ($5x10^5$/mL, B) and high ($1.6x10^7$/mL, **C**) culture density. D**)** Bar graph quantitation of RFP induction by 1mM $CuSO_4$ and by high cell density. The total RFP fluorescence level is calculated as percentage of RFP positive cell multiplied by mean RFP intensity of the cell population. Left two bars, untransfected S2 cells at low density ($5x10^5$/mL) and high density ($1.6x10^7$/mL), respectively. Third Bar, MR cells at low density incubated for 24 hours with 1mM $CuSO_4$. The RFP level in these cells is used as 1 to calculate fold of induction. Right bar, MR cells at high density ($1.6x10^7$/mL) in the absence of $CuSO_4$. E-F) LacZ reporter induction by high cell density in S2 cells. E.) Schematic of the MT-LacZ (MZ) transgene. Transgene components are shown as in Figure 1 except the LacZ coding region is shown in blue. F**)** Bar graph quantitation of LacZ induction by high cell density. LacZ reporter level is quantitated (see method for details). Left two bars, LacZ level in untransfected S2 cells at low density ($5x10^5$/mL) and high density ($1.6x10^7$/mL), respectively. Third bar, LacZ level of MZ cells at low cell density ($5x10^5$/mL). The LacZ level in these cells is used as 1 to calculate fold of induction. Right bar, LacZ level of MZ cells at high density ($1.6x10^7$/mL). G**)** Bar graph comparison of GFP induction by high cell density in *Drosophila* S2 and Kc cells containing the MG transgene. Left two bars, GFP level in MG-containing S2 cells at low density ($5x10^5$/mL) and high density ($1.6x10^7$/mL), respectively. Right two bars, GFP level in MG-containing Kc cells at low density ($5x10^5$/mL) and high density

($1.6x10^7$/mL), respectively. The GFP level in low-density S2 cells is used as 1 to calculate fold of induction.

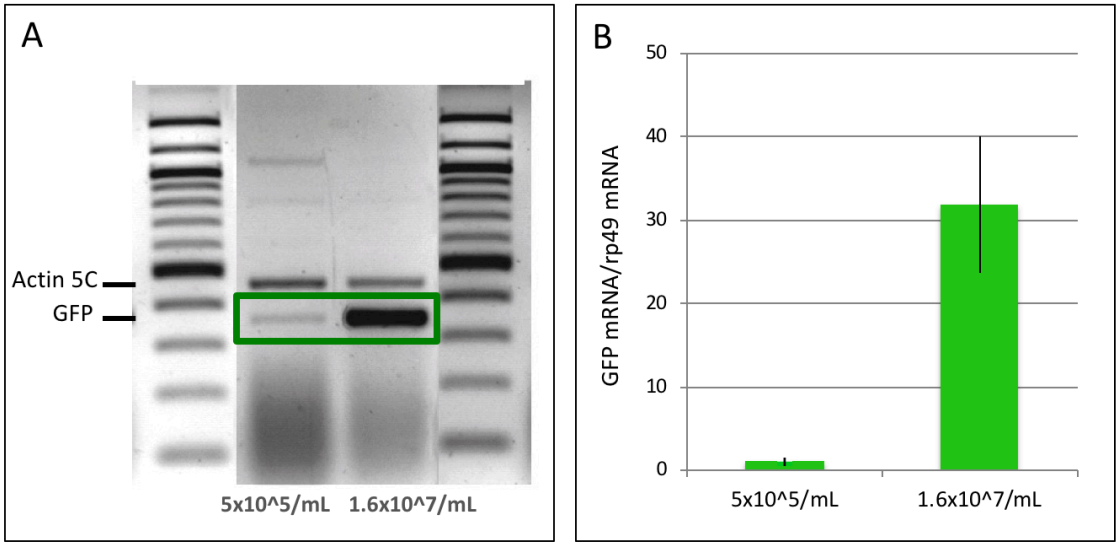
A
Actin 5C
GFP
5x10^5/mL
1.6x10^7/mL
B
GFP mRNA/rp49 mRNA
50
40
30
20
10
0
5x10^5/mL
1.6x10^7/mL

Figure 2.3

Figure 2.3 Crowding induction of GFP occurs at the mRNA level

A) Photo of agarose gel electrophoresis of multiplex RT-PCR product (see methods for detail). Left and right lanes, DNA size marker 100 bp ladder. Center lanes, PCR product from equal number of MG-S2 cells at low density ($5x10^5$/mL, center left) and at high density ($1.6x10^7$/mL, center right). The position of expected Actin 5C (control) and GFP mRNA products are indicted on left. B) Bar graph of GFP RT-PCR product quantitation using a BioRad gel imager. The product mount from the low-density culture is used as 1 to calculate fold of induction.

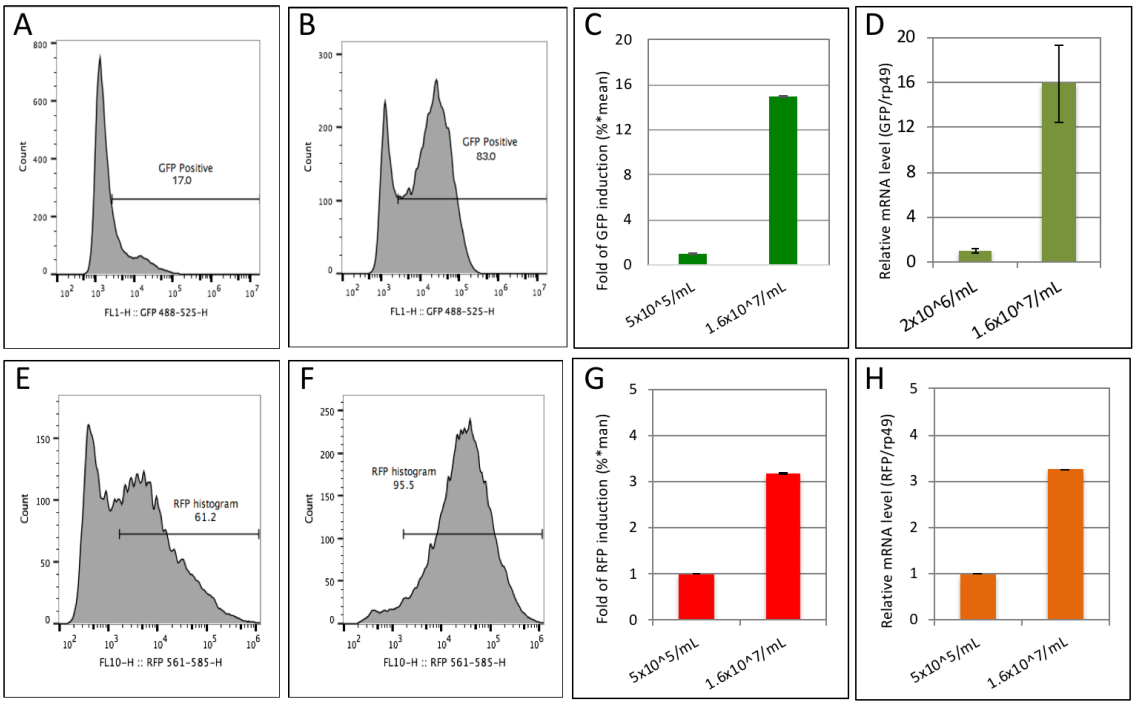
A
B
C
D
E
F
G
H
Count
GFP Positive
17.0
GFP Positive
83.0
FL1-H :: GFP 488-525-H
Fold of GFP induction (%*mean)
Relative mRNA level (GFP/rp49)
5x10^5/mL
1.6x10^7/mL
2x10^6/mL
RFP histogram
61.2
RFP histogram
95.5
FL10-H :: RFP 561-585-H
Fold of RFP induction (%*man)
Relative mRNA level (RFP/rp49)

Figure 2.4

Figure 2.4: Crowding induction of GFP and RFP reporters in S2 cells containing stably integrated transgenes.

A-B) FACS histogram of MG-containing stable cells at low ($5x10^5$/mL, **A**) and high ($1.6x10^7$/mL, **B**) culture density. X-axes: log scale of GFP level; Y-axis: cells number at indicated GFP level. Horizontal bar: GFP positive cells with fluorescence level above $2.5x10^3$. **C.** Bar graph quantitation of crowding induction of GFP protein by FACS. The total GFP fluorescence level is calculated as the percentage of the GFP positive cells multiplied by mean GFP intensity of these cells. The total GFP level in low-density cells is used as 1 to calculate fold of induction. **D.** Bar graph quantitation of crowding induction of GFP mRNA by qRT-PCR using rp49 as a control (see methods for details). The GFP/rp49 mRNA ratio in low-density cells is used as 1 to calculate fold of induction. **E-H.** FACS histogram of MR-containing stable cells at low ($5x10^5$/mL, **E**) and high ($1.6x10^7$/mL, **F**) culture density. X-axes: log scale of RFP level; Y-axis: cells number at indicated RFP level. Horizontal bar: RFP positive cells with fluorescence level above $2.5x10^3$. **G.** Bar graph quantitation of crowding induction of RFP protein by FACS. The total RFP fluorescence level is calculated as the percentage of the RFP positive cells multiplied by mean RFP intensity of these cells. The total RFP level in low-density cells is used as 1 to calculate fold of induction. **H.** Bar graph quantitation of crowding induction of RFP mRNA by qRT-PCR using rp49 as a control (see methods for details). The RFP/rp49 mRNA ratio in low-density cells is used as 1 to calculate fold of induction.

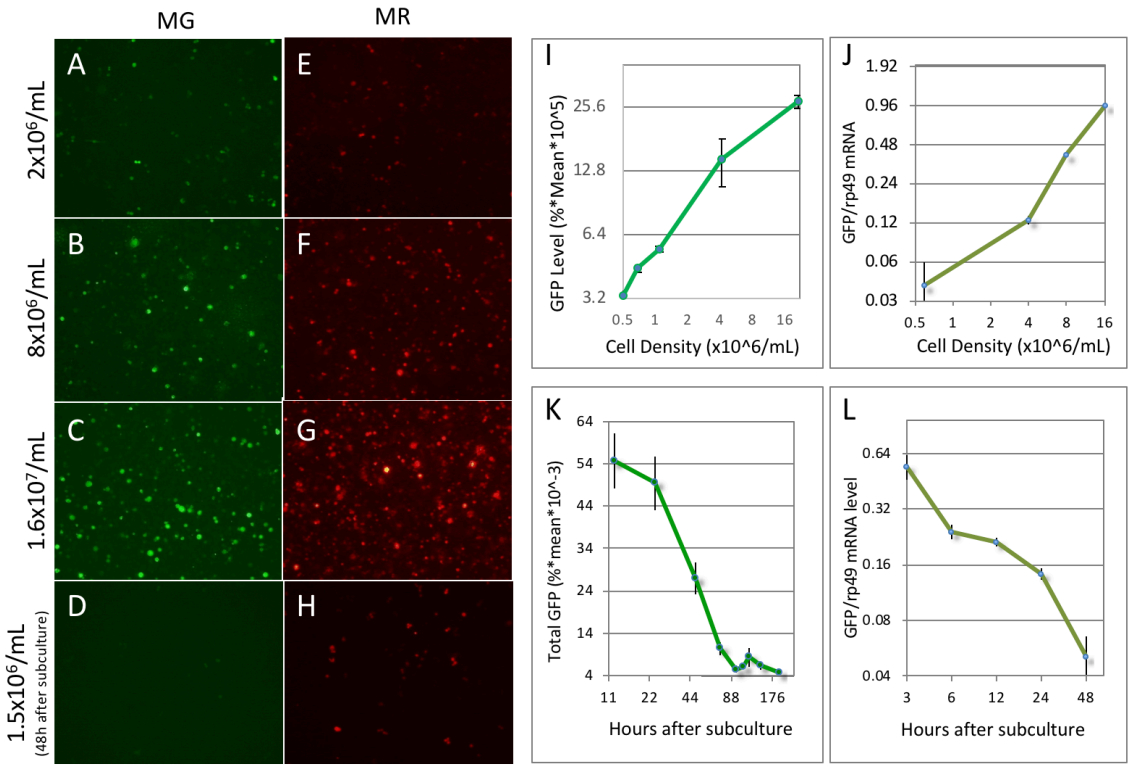
MG
MR
A
E
B
F
C
G
D
H
2x10^6/mL
8x10^6/mL
1.6x10^7/mL
1.5x10^6/mL
(48h after subculture)
I
GFP Level (%*Mean*10^5)
25.6
12.8
6.4
3.2
0.5 1 2 4 8 16
Cell Density (x10^6/mL)
J
GFP/rp49 mRNA
1.92
0.96
0.48
0.24
0.12
0.06
0.03
0.5 1 2 4 8 16
Cell Density (x10^6/mL)
K
Total GFP (%*mean*10^-3)
64
54
44
34
24
14
4
11 22 44 88 176
Hours after subculture
L
GFP/rp49 mRNA level
0.64
0.32
0.16
0.08
0.04
3 6 12 24 48
Hours after subculture

Figure 2.5

Figure 2.5. Reporter induction is cell concentration dependent and reversible.

A-H**.** Representative fluorescent microscope images of stable MG (A-D) and MR (E-H) cells at increasing cell concentration as indicated (A-C, E-G), and 48 hours after subculture from high cell density (D, H), respectively. I-J**.** Quantitation of GFP levels at increasing cell concentrations as indicated. The total GFP fluorescence level, as measured by FACS, is calculated as the percentage of the GFP positive cells multiplied by mean GFP intensity (**I**). The GFP mRNA, as measured by qRT-PCR, is calculated as the ratio of GFP mRNA/rp49 mRNA (**J**). K-L**.** GFP fluorescence (K) and mRNA (L) levels after increasing length of time post subculture.

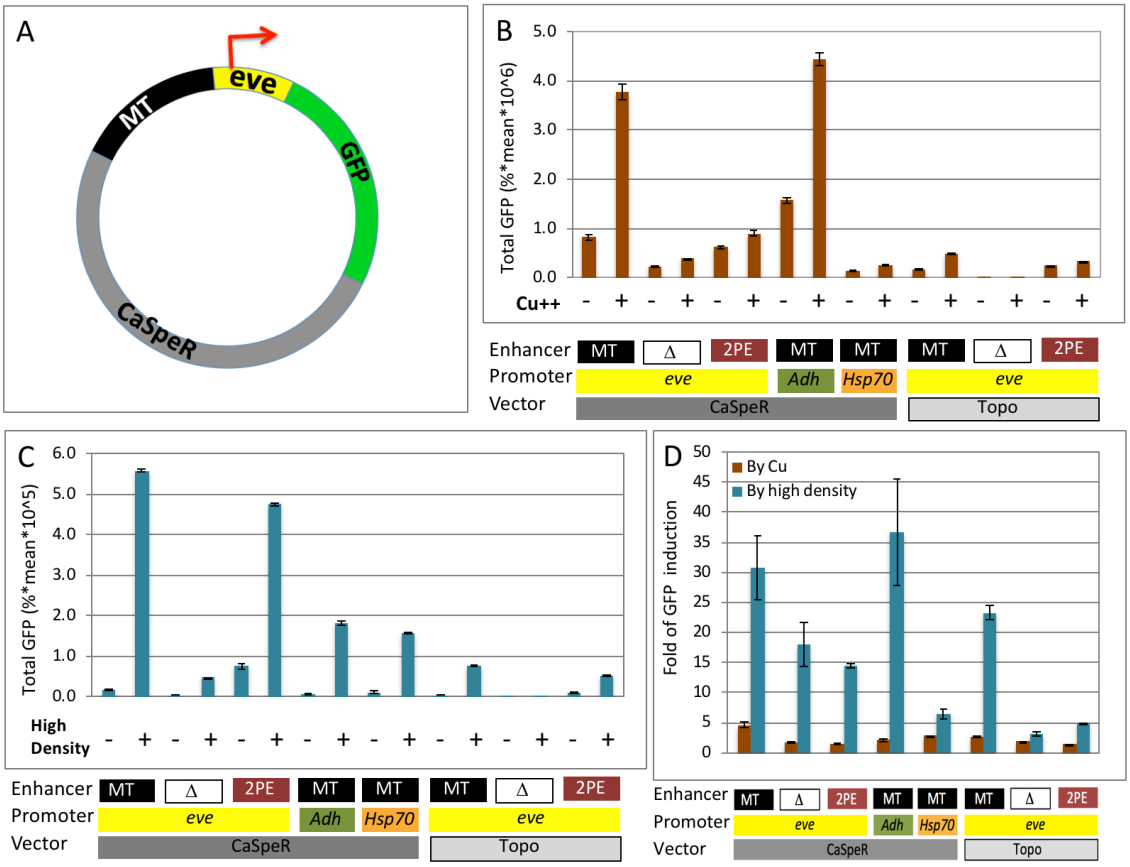
A
MT
eve
GFP
CaSpeR
B
Total GFP (%*mean*10^6)
5.0
4.0
3.0
2.0
1.0
0.0
Cu++
- + - + - + - + - + - + - + - +
Enhancer
Promoter
Vector
MT
Δ
2PE
eve
Adh
Hsp70
CaSpeR
Topo
C
Total GFP (%*mean*10^5)
6.0
5.0
4.0
3.0
2.0
1.0
0.0
High Density
- + - + - + - + - + - + - + - +
D
Fold of GFP induction
By Cu
By high density
50
45
40
35
30
25
20
15
10
5
0

Figure 2.6

Figure 2.6. Multiple components in the transgene sequences contribute to density-mediated reporter induction.

A. Schematic of the MT-GFP (MG) transgene as in Figure 1A. Transgene components are shown in different colors: CaSpeR vector (grey), MT enhancer (black), *evenskipped* basal promoter (light yellow) and the GFP reporter gene (green). The red arrow: Transcription start site (+1). **B.** The MT enhancer is responsible for Cu^{++}-mediated reporter activation. GFP levels are quantitated by FACS in S2 cells containing transgenes with different enhancers, promoters and vectors sequences, as indicated, in the presence (+) and absence (-) of 1mM $CuSO_4$. **C.** The MT and 2PE enhancers both mediate crowding-induced reporter activation. GFP levels are quantitated by FACS in S2 cells containing transgenes with different combinations of enhancers, promoters and vectors sequences, as indicated, in low ($5x10^5$/mL, -) or high ($1.6x10^7$/mL, +) cell density. **D.** Differential reporter induction by $CuSO_4$ and cell crowding in S2 cell containing different transgenes. Fold of GFP induction by 1mM $CuSO_4$ over uninduced (brown bars) and by high cell density over low density (blue bars) are shown for transgenes containing different combinations of enhancers, promoters and vectors sequences, as indicated.

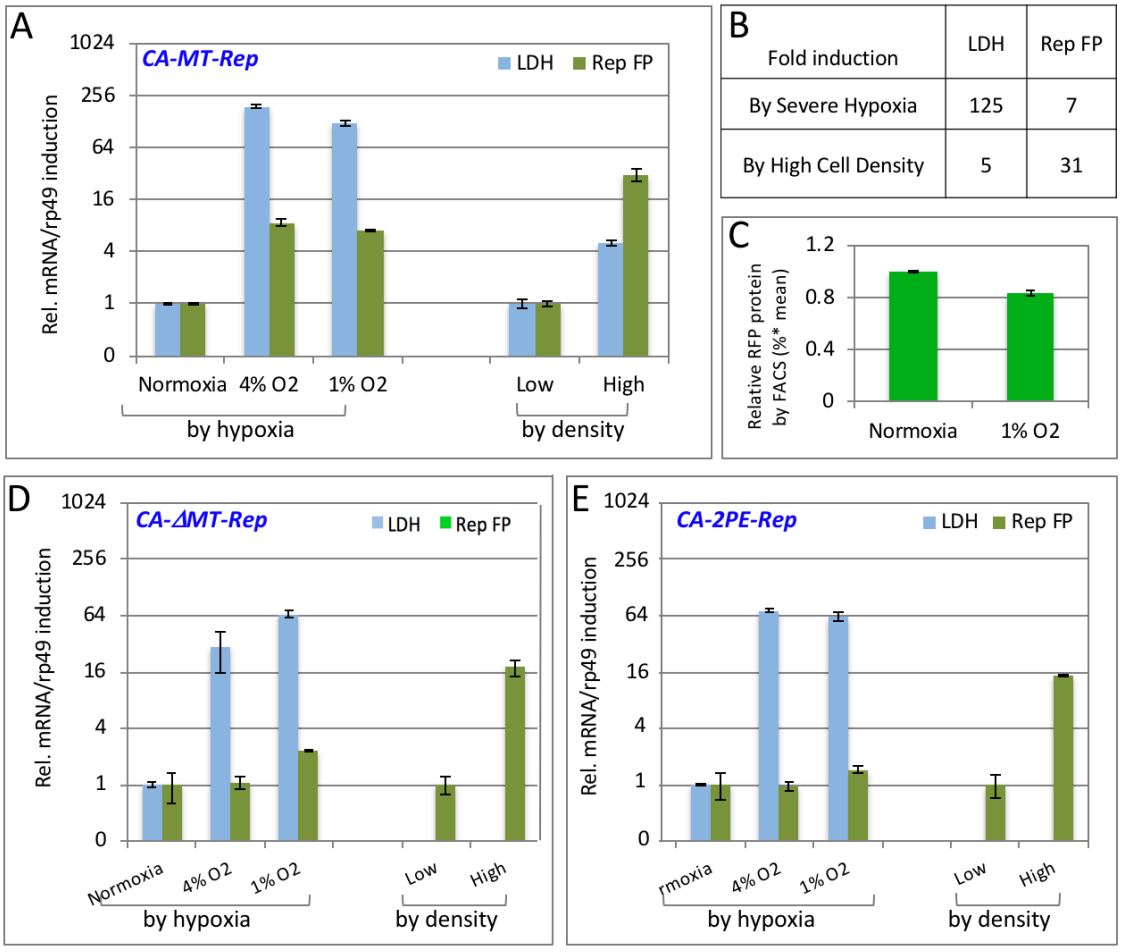
A
CA-MT-Rep
LDH
Rep FP
Rel. mRNA/rp49 induction
1024
256
64
16
4
1
0
Normoxia
4% O2
1% O2
Low
High
by hypoxia
by density
B
Fold induction
LDH
Rep FP
By Severe Hypoxia
125
7
By High Cell Density
5
31
C
Relative RFP protein by FACS (%* mean)
1.2
0.8
0.4
0
Normoxia
1% O2
D
CA-ΔMT-Rep
LDH
Rep FP
Rel. mRNA/rp49 induction
1024
256
64
16
4
1
0
Normoxia
4% O2
1% O2
Low
High
by hypoxia
by density
E
CA-2PE-Rep
LDH
Rep FP
Rel. mRNA/rp49 induction
1024
256
64
16
4
1
0
rmoxia
4% O2
1% O2
Low
High
by hypoxia
by density

Figure 2.7

Figure 2.7. Hypoxia partially contribute to reporter mRNA induction but not protein induction.

A**)** Quantitation of relative LDH (blue) and GFP (green) mRNA induction by hypoxia (left) and by high cell density (right) in MG transfected cells. The LDH/rp49 or GFP/rp49 mRNA ratio in low-density non-hypoxic cells is used as 1 to calculate fold of induction. B**)** Summary of relative fold of induction of GFP mRNA by severe (1% O_2) and by high ($1.6x10^7$/mL) cell density. C) FACS quantitation of the relative GFP protein level under severe hypoxia (1% O_2). The total GFP level in low-density, non-hypoxic cells, from multiplying percentage of the GFP positive cells and mean GFP intensity, is used as 1 to calculate fold of induction. D) Quantitation of relative LDH (blue) and GFP (green) mRNA induction by hypoxia (left) and by high cell density (right) in ΔMT transfected cells. The LDH/rp49 or GFP/rp49 mRNA ratio in low-density non-hypoxic cells is used as 1 to calculate fold of induction. E**)** Quantitation of relative LDH (blue) and GFP (green) mRNA induction by hypoxia (left) and by high cell density (right) in 2PE transfected cells.

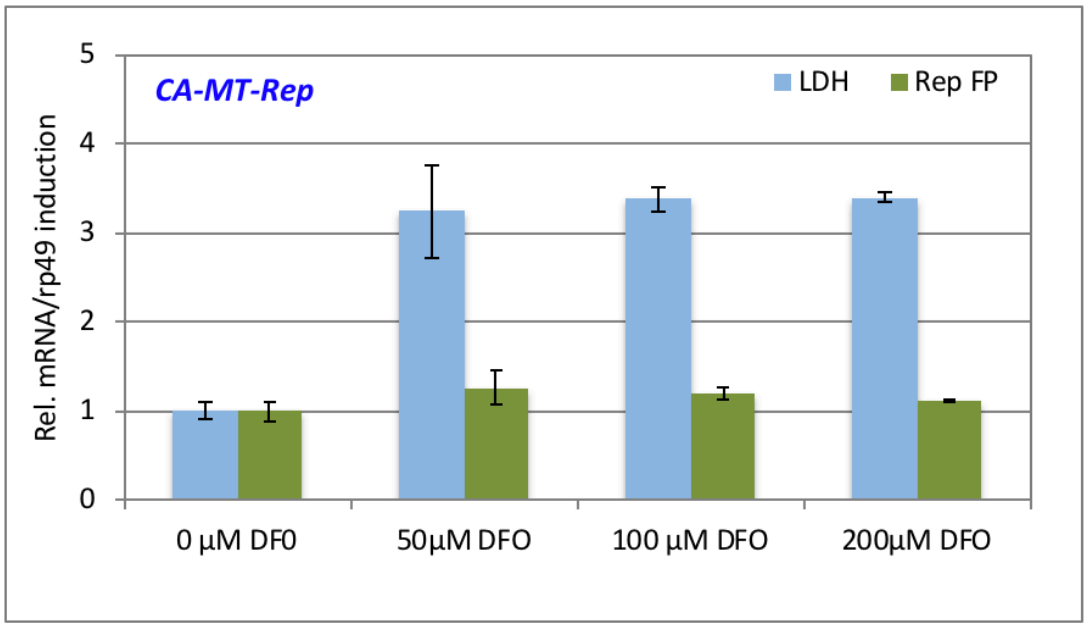
CA-MT-Rep
LDH
Rep FP
Rel. mRNA/rp49 induction
5
4
3
2
1
0
0 µM DF0
50µM DFO
100 µM DFO
200µM DFO

Figure 2.8

Figure 2.8 GFP reporter is not induced by up to 200 mM DFO. Quantitation of relative

LDH (blue) and GFP (green) mRNA induction by increasing concentration of DFO (from left to right) in MG transfected cells. The LDH/rp49 or GFP/rp49 mRNA ratio in low-density, 0 μM DFO cells is used as 1 to calculate fold of induction.

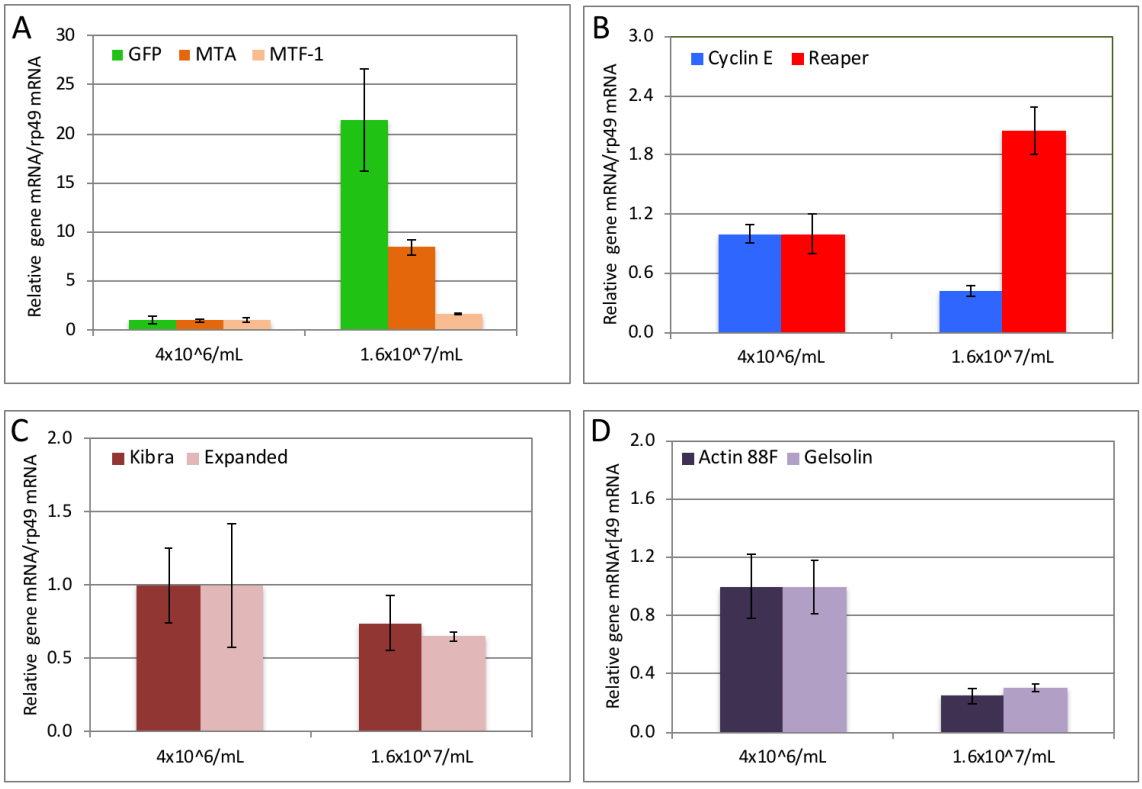
A
GFP
MTA
MTF-1
Relative gene mRNA/rp49 mRNA
30
25
20
15
10
5
0
4x10^6/mL
1.6x10^7/mL
B
Cyclin E
Reaper
Relative gene mRNA/rp49 mRNA
3.0
2.4
1.8
1.2
0.6
0.0
4x10^6/mL
1.6x10^7/mL
C
Kibra
Expanded
Relative gene mRNA/rp49 mRNA
2.0
1.5
1.0
0.5
0.0
4x10^6/mL
1.6x10^7/mL
D
Actin 88F
Gelsolin
Relative gene mRNAr[49 mRNA
2.0
1.6
1.2
0.8
0.4
0.0
4x10^6/mL
1.6x10^7/mL

Figure 2.9

Figure 2.9 Changes in multiple signaling pathways correlates with reporter expression during cell proliferation

A-D. Relative gene expression of components of GFP and the MTA pathway (A), cell cycle and apoptosis pathway (B), Hippo pathway (C) and cytoskeletal components (D) at medium ($4x10^6$/mL) and high ($1.6x10^7$/mL) cell density. Gene names are indicated on top of chart and gene mRNA/rp49 mRNA ratio at medium density is used as 1 to calculate fold of induction.

Gene	Forward primer 5'-3'	Reverse primer 5'-3'
ML hsp70 promoter 1.6k	GCGGCCGCGAGAGCTTTGCAGACT	GGATCCGTTTAGCTTGTTCAGCTG
ML Adh promoter 1.4k	GCGGCCGCGATTGATTCTACGCTG	GGATCCTGACTTCTTTTTTGCTTTAG
GFP RT	TGACCCTGAAGTTCATCTGCACCA	TTGATGCCGTTCTTCTGCTTGTCG
RFP RT	ACTACTTGAAGCTGTCCTTCCC	CCCATGGTCTTCTTCTGCATTAC 3'FOR RFP
rp49 RT	CGATATGCTAAGCTGTCGCAC	GGTTCTGCATGAGCAGGAC
MT-A RT	CAACTCAATCAAGATGCCTTGCC	AGCGCCTCTACTCCAGATC
MTF-1 RT	ATTCAACACGCGCTACAGATTG	TGAACTCCTCTTCCTCTTGCT
Cyclin E RT	GCAGCGATTCAAACGAGCTG	GTGAGCTACGTATGCTGAGC
Reaper RT	CAACAATGGCAGTGGCATTC	TCCTCATTGCGATGGCTTG
Merlin RT	CAGGACCTCCACATCAACAAA	CTCTTCGGAACGCCGTTC
Kibra RT	GCCAGTCGAAGCAGTCTGTG	CGACTTGTGCACCTTGAGC
Actin 88F RT	TCTGGACTTCGAGCAGGAGAT	GACAGCACAGAGTTGGCATACA
Gelsolin RT	GAGCTATTTCAAAAACGGCATTCG	TAGCTTCTCAACGCGCTTG

Table 2.1

CHAPTER 3

INVESTIGATING THE NATURE OF CROWDING MEDIATED INDUCTION IN A POSSIBLE S2 CELL DENSITY SENSING SYSTEM

3.1 Abstract

Cell density sensing is an important mechanism that is involved in development, wound healing, and when misregulated cancer. There still remains many gaps in knowledge about how density sensing is done. We have discovered a transgenic fluorescent reporter system that is responsive to changes in cell density. Here we investigated the nature of this crowding induction to determine what stimulus from cell crowding activates the reporter. We have found that forcing the transgenic cells into contact induces a relatively quick reporter induction that does not require a new round of transcription. This response does not appear to be caused by any sort of diffusible factor. The cells' attachment to the extracellular membrane (ECM) has no effect on reporter induction as well. We found that the only other means of reporter induction besides forcing the cells into direct contact occurs when the transgenic line is close proximity to a crowded cell culture with a polycarbonate membrane separating the cell bodies in between the two cultures. Our results indicate that the crowding induced reporter is cell density dependent and distance dependent suggesting a necessity for membrane contact that may be mediated by cytonemes.

3.2 Introduction

Density sensing is an important cellular mechanism that helps organisms with development, tissue growth, and wound healing. When misregulated there can be improper tissue formation (i.e. stem cell differentiation) and tumor formation. *Drosophila* has been a major pioneer in density sensing pathways. The Hippo pathway, a signaling pathway that can modulate cell division based on cell density, was discovered in *Drosophila* first and later found to be conserved in mammals, *C. elegans*, and yeast. Other cell density based pathways such as caspase mediated cell elimination and Piezo1 stretch induced proliferation have also been studied in *Drosophila*. Many parallel studies on density sensing and its cellular effects have been carried out in other models, but despite this there is still much unknown about how cell density sensing is regulated and what impact it can have on cells.

Our lab has discovered a transgenic reporter S2 cell culture system that has exhibits an increase in the expression of a fluorescent reporter in response to an increase in cell density. S2 cells are macrophage like cells derived from a *Drosophila* embryo and have been used in many synthetic biology experiments to determine a molecule's function [4]. This includes cell studies for the Hippo density sensing pathway [151, 152]. S2 cells' features allow for them to be easily cultured and great tools for RNAi studies and fluorescent microscopy studies [3, 6, 153]. Here we sought to determine the cellular stress(es) responsible for the cell crowding mediated reporter induction in our transgenic S2 cell system in an effort to validate it as a useful platform for cell density sensing. Using the reporter expression as a readout for induction, we manipulated when cells experience cell to cell contact, the cells' environment, and the distance between

populations of cells to find that cell to cell contact is most likely responsible for increased reporter expression and that the cell contact might be mediated by cytonemes.

3.3 Results and Discussion

Forcing sparse cells into contact induces reporter expression

It was previously shown that the increase in reporter expression occurs from an increase in mRNA and can also be seen in an increase in protein level, indicated by detecting fluorescence level per cell. The cause of the increase in reporter expression was found to be cell density dependent and largely hypoxic independent. We began by testing if forcing the reporter cells into contact would cause reporter induction. We did this by growing up large quantities of sparse reporter cells, that are dark and not expressing the reporter, then concentrated them in a centrifuge for subsequent re-suspension in fresh media and seeding into a new smaller culture dish. We refer to this process as artificial crowding. (Fig. 3.1A) We first examined how artificial crowding to a density we have previously seen the cells grow to (12million/mL) and observed a high level of reporter expression (16x induction over sparse). We observed comparable levels of reporter induction both on a mRNA and protein level. (Fig. 3.1B, C) This level of induction was also dependent on the density that the cells were artificially crowded to which matches previous data showing that the natural ramp-up of induction is correlated with the natural increase of density. (Fig. 3.1C) Interestingly, when examining dynamics we observe a rather rapid induction take place from artificial crowding that starts around 3hrs after being artificially crowded. (Fig. 3.1B, C) This rate is faster than the S2 cell division rate of 22hrs and is similar to times for cellular responses seen in some of the other density

sensing pathways such as Hippo and Piezo1 [6, 20, 48]. In addition to this, the artificial crowding reporter expression appears to be a direct result of the signal responding to the change in cell density and does not require a new round of translation prior to transcribing the reporter gene. This is seen by the expression of the reporter gene after artificial crowding while the cells were being incubated with the Cyclohexamide drug that inhibits translation. (Fig. 3.1 D) The artificial crowding experiments suggests that simply forcing the cells into contact can induce the transgene and that it is unlikely due to any sort of nutrient deprivation since the induction takes place in fresh fully supplemented media.

Crowding induction is not mediated by a soluble factor

The secretome is a form of proteomics that focuses on proteins that are released from a cell into the environment which can include a wide array of proteins from cytokines, growth factors, to ECM components and more [154, 155]. The secretome for a cell is found in the media that the cells are cultured in and is referred to as conditioned media [154, 156]. The effects of conditioned media on cells has been looked at for many decades, and studies have shown conditioned media to have growth inhibiting, growth promoting, healing, and differentiation promoting behavioral effects [156, 157]. We decided to examine whether the crowding mediated reporter induction was brought about by the presence of a secreted factor that might be newly present or simply highly concentrated in dense S2 cell culture. We collected the conditioned media from untransfected S2 cells that were grown to very dense conditions which has been associated with high expression of the reporter. (Fig. 3.2A) We first incubated sparse

reporter cells with conditioned media to see if it would induce reporter expression and saw no change in GFP protein level. (Fig. 3.2B) We also examined whether conditioned media would have an affect on the reporter cells if they were in a more crowded state. We tested this by letting the reporter cells grow to confluence, approximately 6mil/mL density where all of the cells have grown to form a monolayer and has an intermediate reporter expression, then changing their media for either conditioned media or fresh media. (Fig. 3.2A) We observed was that the introduction of fresh media led an increase of reporter induction compared to fresh media which could be attributed to a higher cell number and division rate. We also tried another source of conditioned media that would provide a more nutrient rich source than the previous conditioned media, so we tried using the media from artificially crowded cells which have been shown to have reporter induction as the source. We found that again there was no induction in sparse reporter cells with the artificially crowded conditioned media after 12hrs of incubation. (Fig. 3.2C) We also checked to see if the reporter induction could be caused by a secreted factor with a short half-life by checking reporter expression level after a short incubation of 3hr with the artificially crowded conditioned media. (Fig. 3.2C) There was no significant change in reporter induction seen.

From incorporation of conditioned media to study the sectretome's effect on reporter induction, we conclude that it is likely that there is not a secreted factor responsible for the crowding mediated reporter induction. In addition, the use of conditioned media from naturally crowded cells, where the nutrient content would be low, implies that a lack of soluble nutrients may not be the cause of crowding reporter induction.

Reporter expression requires dense cells in close proximity

Our previous results indicate that the cell crowding reporter induction we see occurs when cell density increases and is not a result from a lack of nutrients or a secreted factor. Two other changes cells experience during repeated divisions are a decrease in cell surface area and cell to ECM attachment surface and an increase in cell to cell contact surface. S2 cells have been documented to have a little endogenous α-integrin expression and to attach to cell culture dishes [4, 158]. Culturing S2 cells without serum, we have observed cell attachment to the tissue culture dishes that can be overcome by blowing off the cells with a pipet. When the cells are sparse and the reporter expression is low in the transgenic cells, the cells are attached and spread out across the cell culture dish exhibiting a fibroblast shape. (Fig. 2.1B) To determine if attachment and the stretched cell morphology was necessary for maintaining a dark cell state in the reporter cell line, we used agarose to prevent cell attachment and force them to remain in suspension a technique commonly used for anoikis and 3D cell culture studies [159, 160]. When sparse reporter cells were seeded on an agarose covered culture dish, they clustered and floated in suspension. The loss of attachment for the sparse reporter cells had no influence on the reporter induction. This indicates that attachment to the culture plate and the stretched cell morphology likely had no influence on the crowding reporter induction seen.

This led us to investigate cell-cell contact as the mediator of the crowding reporter induction. Examination of the S2 cell membrane has shown that the membrane has cytoskeletal projections [161, 162]. We examined the S2 cells ourselves using TIRF and

DIC microscopy and also observed cytoskeletal projections that look like filopodia. (Fig. 3.3B) A recent study has classified these filopodia as cytonemes, meaning that they are thin actin driven cytoskeletal projections capable of transporting morphogens [162]. We used a transwell insert that can separate two cell bodies in a tissue culture plate. The insert is a polycarbonate membrane that has .4μm pores which is bigger than the documented cytonemes seen in S2 cells [162]. We tested four different conditions to determine if a population of sparse reporter cells could be induced by subset of dense S2 cells. (Fig. 3.3C) Our experiment showed that dense cells can induce reporter expression in the transgenic sparse cells, and that this induction is distance dependent. (Fig 3D) The sparse reporter cells only induced in close proximity to the dense culture which based on the transwell membrane thickness is 10μm - a distance that is smaller than the reported cytoneme length in S2 cells. The inability for the sparse cells from the dense culture to induce the reporter population also suggests that the dense cell state is a transient state and that its effects are observed only while in the highly crowded state.

All together upon further examination of the mechanism of crowding mediated reporter induction in our labs transgenic S2 cells, we have found that the reporter expression is dependent upon cell density and requires cells to be close enough that membrane projections could contact one another. We showed that forcing sparse cells together has a rather rapid induction rate for reporter expression which is similar to the response time of other contact dependent mechanisms. This expression of the reporter from forcing cells into contact does not require a new round of transcription indicating the increase of expression is a direct result from crowding the cells. Through the use of conditioned media we demonstrated that the reporter induction is not due to a soluble

factor secreted from cells in a crowded state. Along with the artificial crowding – which was done in fresh media likely eliminating most nutrient stresses –, our conditioned media experiments also indicate that reporter induction is not a result from a lack of nutrients. Removal of substrate for the reporter cells to attach to by using agarose caused the cells to remain in suspension, and this loss of cell to ECM attachment had no effect on reporter induction. This indicates that cell-ECM attachment and also cell polarity are not crucial in our crowding mediated induction. Our findings and recent reports of S2 cytoskeletal projections show that cytonemes are present and that they could serve as means of communication. With the use of a transwell insert - which has pores large enough for most soluble molecules and cytonemes to pass through, we found that dense S2 cells can induce sparse reporter cells to express the reporter, but that this induction was distance dependent. In our case the sparse reporter cells must be within 10μ for the inducing effects of the dense S2 cell culture to be effective – a range that is within the reach of cytonemes. Further examination regarding the nature of contact required for the reporter cell line to induce reporter expression needs to be done, and our lab is currently in the process of generating a monoclonal fluorescent reporter to use for sensitive microscopy studies. However our current findings investigating the mechanism of the crowding mediated induction seen in the transgenic S2 cells indicate that it may serve as useful platform for future studies related to cell to cell contact and cell density sensing mechanisms.

Methods

S2 cell Culture

Drosophila Schneider's Line 2 (S2) cells were maintained in HyQ SFX-Insect serum-free medium (HyClone) at 25°C. Cells were sub-cultured every 6 days.

Flow cytometry and imaging

Fluorescence Activated Cell Sorting was performed using Cytoflex flow cytometer (Beckman Coulter). Briefly, cells were washed off the plate and taken to the cytometer. Twenty thousand cells were analyzed for each sample. Fluorescence was excited at 405nm and 56nm . The photomultiplier detection voltages were set at 400 V for FL1 and 375 V for FL2. Data analysis was done using the Flojo software. Green fluorescence was detected with FL1 530/30 BP filter; red fluorescence was detected with FL2 585/42 BP filter. G/RFP level, is calculated as: [% of G/RFP positive cells (>10) × mean GFP fluorescence]. For all quantitation graphs, the error bar is calculated as: SEM = standard deviation (SD)/square root [replicate number (N)]. Images were taken with custom-built TIRF/epi-fluorescence structure-illumination microscope (TESM) and Epifluorescence imaging was done on an Axioskop II plus microscope with a 100x Plan-Apochromat 1.4 NA objective and a digital charge-coupled device MrM camera (Carl Zeiss, Inc.).

RT-qPCR

RNA extraction performed using TRIZOL reagent (invitrogen). cDNA library was generated using oligo-d(T) primer and superscript III (Invitrogen). cDNA library was used in qPCR analysis to quantify gene expression using SYBR Green Supermix (Bio-Rad). The following primers were used: 5’ tgaccctgaagttcatctgcacca 3’ and 5’

ttgatgccgttcttctgcttgtcg 3’ for GFP; 5’ actacttgaagctgtccttccc 3’ and 5’ cccatggtcttcttctgcattac 3’for RFP

Figure 3.1

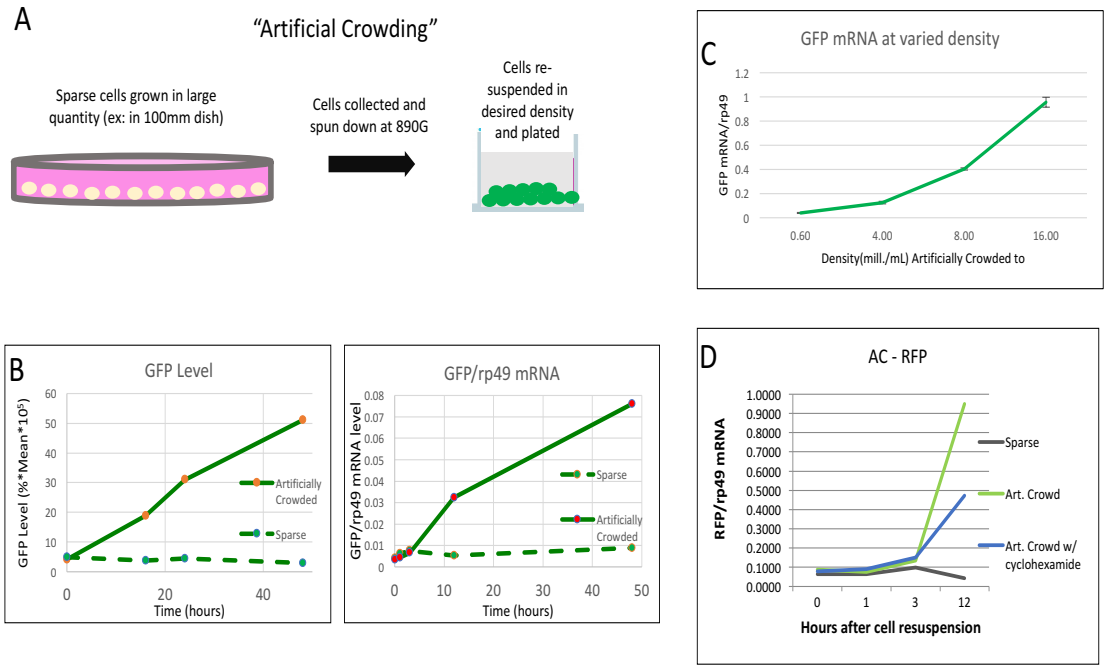
A
"Artificial Crowding"
Sparse cells grown in large quantity (ex: in 100mm dish)
Cells collected and spun down at 890G
Cells re-suspended in desired density and plated
C
GFP mRNA at varied density
GFP mRNA/rp49
Density(mill./mL) Artificially Crowded to
B
GFP Level
GFP Level (%*Mean*10⁵)
Artificially Crowded
Sparse
Time (hours)
GFP/rp49 mRNA
GFP/rp49 mRNA level
Sparse
Artificially Crowded
Time (hours)
D
AC - RFP
RFP/rp49 mRNA
Sparse
Art. Crowd
Art. Crowd w/ cyclohexamide
Hours after cell resuspension

Figure 3.1 Forcing sparse cells into contact induces reporter expression

A)Graphical abstract of artificial crowding process. Sparse transgenic cells are grown up in a sparse density to retain low levels of reporter expression. Once enough cells are acquired, the cells are blown off of the plate with a pipetman to be collected, concentrated, and re-plated B)GFP protein level from FACS and mRNA level over the course of 48hrs for MG cells artificially crowded to 12million/mL C)GFP mRNA level 12hrs after MG cells have been artificially crowded to the specified density D)RFP mRNA level for MR cells artificially crowded to 12mil/mL and treated with cyclohexamide

Figure 3.2

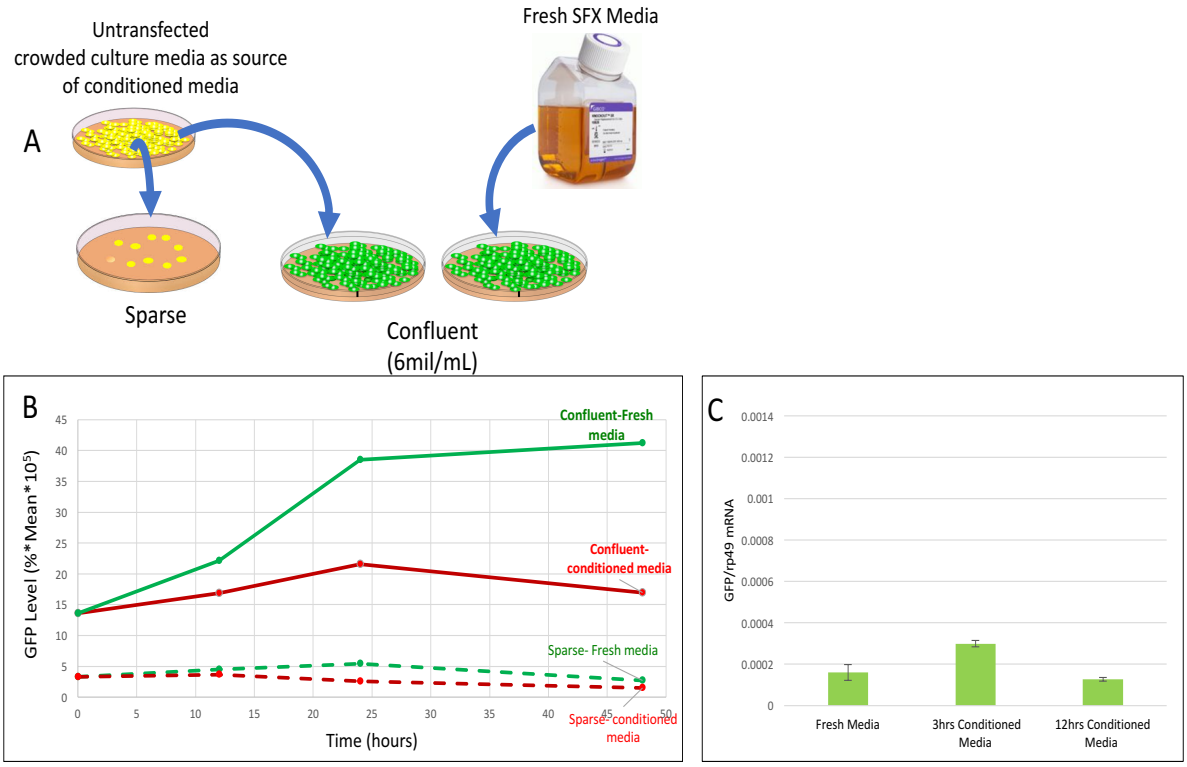
A
Untransfected
crowded culture media as source
of conditioned media
Fresh SFX Media
Sparse
Confluent
(6mil/mL)
B
GFP Level (%*Mean*10⁵)
Time (hours)
Confluent-Fresh media
Confluent-conditioned media
Sparse- Fresh media
Sparse- conditioned media
C
GFP/rp49 mRNA
Fresh Media
3hrs Conditioned Media
12hrs Conditioned Media

Figure 3.2 Crowding induction is not mediated by a diffusible factor

A)Graphical abstract of conditioned media experiment. Conditioned media was obtained from dense S2 cells (16mil/mL) that were grown for 6 days. Media was then removed from the S2 cells to be added to both sparse and confluent MG cells. A separate confluent well had its media removed and fully replaced with fresh media. B)GFP protein level was measured using FACS over the course of 48hrs for the sparse and confluent cells incubated with fresh media and the S2 cell conditioned media. C)GFP mRNA level measured on sparse MG cells with fresh media or conditioned media from artificially crowded cells. mRNA measurements were done after 12hrs of incubation with fresh media, and a 3hr or 12hr incubation with the conditioned media

Figure 3.3

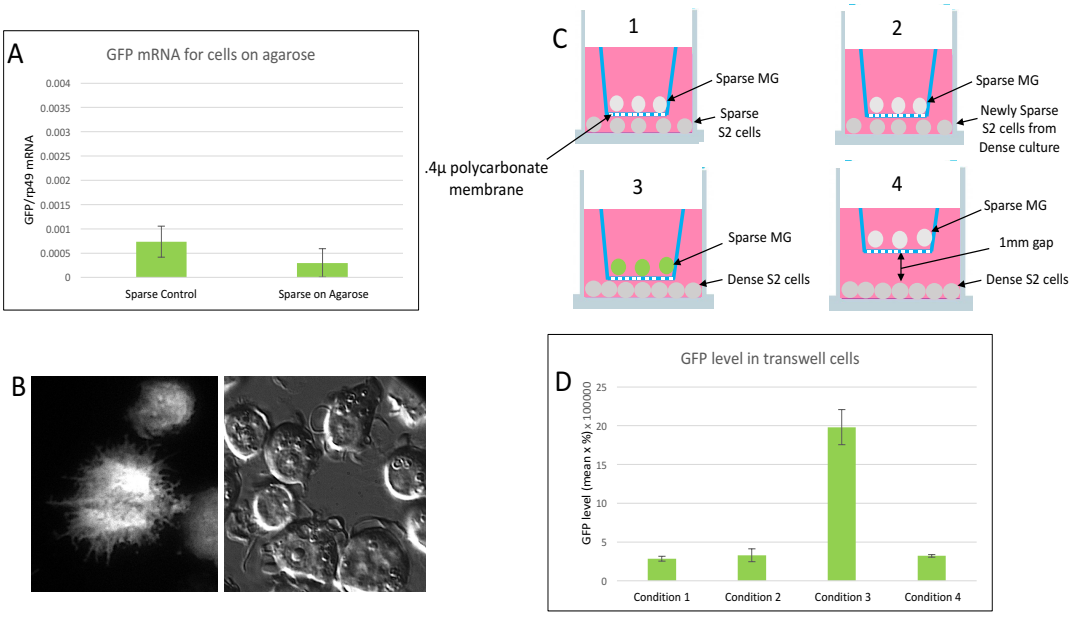
A
GFP mRNA for cells on agarose
GFP/rp49 mRNA
0.004
0.0035
0.003
0.0025
0.002
0.0015
0.001
0.0005
0
Sparse Control
Sparse on Agarose
B
C
1
Sparse MG
Sparse S2 cells
.4µ polycarbonate membrane
2
Sparse MG
Newly Sparse S2 cells from Dense culture
3
Sparse MG
Dense S2 cells
4
Sparse MG
1mm gap
Dense S2 cells
D
GFP level in transwell cells
GFP level (mean x %) x 100000
25
20
15
10
5
0
Condition 1
Condition 2
Condition 3
Condition 4

Figure 3.3 Reporter expression requires dense cells in close proximity

A)GFP mRNA level on MG cells plated on agarose for 16hrs/overnight. The control is sparse cells on traditional polystyrene tissue culture plate. B)Tirf and DIC images of reporter S2 cells. C)Graphical abstract of the transwell insert experiment: the transwell insert held sparse MG cells over variable culture conditions and the MG cells inside the transwell were measured for reporter protein level. Condition 1) sparse S2 cells on the bottom of the well; the transwell is sitting directly on the sparse S2 cells. Condition 2) Sparse cells that came directly from a dense S2 cell culture on the bottom of the well; the transwell is directly on the sparse S2 cells. Condition 3) dense S2 cells on the bottom of the well; transwell is directly on the dense S2 cells. Condition 4) Dense S2 cells on the bottom of the well; the transwell is 1mm above the dense cells on the bottom of the well. D)Results of transwell experiment. Reporter level was measured using FACS.

References:

1. Abercrombie, M. and J.E.M. Heaysman, *Observations on the social behaviour of cells in tissue culture: II. "Monolayering" of fibroblasts.* Experimental Cell Research, 1954. **6**(2): p. 293-306.
2. Martz, E. and M.S. Steinberg, *The role of cell-cell contact in 'contact' inhibition of cell division: A review and new evidence.* Journal of Cellular Physiology, 1972. **79**(2): p. 189.
3. Buster, D.W., et al., *Preparation of Drosophila S2 cells for Light Microscopy.* Journal of Visualized Experiments : JoVE, 2010(40): p. 1982.
4. Yang, J. and M. Reth, *Drosophila S2 Schneider Cells: A Useful Tool for Rebuilding and Redesigning Approaches in Synthetic Biology*. 2012, HUMANA PRESS: United States. p. 331.
5. Fehon, R.G., et al., *Molecular interactions between the protein products of the neurogenic loci Notch and Delta, two EGF-homologous genes in Drosophila.* Cell, 1990. **61**(3): p. 523-534.
6. Dobbelaere, J., *Chapter 15 - Genome-wide RNAi screens in S2 cells to identify centrosome components*, in *Methods in Cell Biology*, R. Basto and K. Oegema, Editors. 2015, Academic Press. p. 279-300.
7. Toret, C.P., et al., *A genome-wide screen identifies conserved protein hubs required for cadherin-mediated cell–cell adhesion.* The Journal of Cell Biology, 2014. **204**(2): p. 265.
8. Kechad, A. and G.R.X. Hickson, *Chapter 4 - Imaging cytokinesis of Drosophila S2 cells*, in *Methods in Cell Biology*, A. Echard, Editor. 2017, Academic Press. p. 47-72.
9. Lee, H., Y. Peng, and Y. Guo, *Chapter 4 - Analysis of Lipid Droplet Dynamics and Functions in Drosophila melanogaster*, in *Methods in Cell Biology*, H. Yang and P. Li, Editors. 2013, Academic Press. p. 53-69.
10. Meng, Z., T. Moroishi, and K.-L. Guan, *Mechanisms of Hippo pathway regulation.* Genes & Development, 2016. **30**(1): p. 1-17.
11. Li, S., et al., *Overlapping functions of the MAP4K family kinases Hppy and Msn in Hippo signaling.* Cell Discovery, 2015. **1**: p. 15038.
12. Koontz, L.M., et al., *The Hippo effector Yorkie controls normal tissue growth by antagonizing scalloped-mediated default repression.* Developmental cell, 2013. **25**(4): p. 388-401.
13. Oh, H. and K.D. Irvine, *Cooperative Regulation of Growth by Yorkie and Mad through bantam*. Developmental Cell, 2011. **20**(1): p. 109-122.
14. Peng, H.W., M. Slattery, and R.S. Mann, *Transcription factor choice in the Hippo signaling pathway: homothorax and yorkie regulation of the microRNA bantam in the progenitor domain of the Drosophila eye imaginal disc.* Genes & development, 2009. **23**(19): p. 2307-2319.
15. Bae, S.J., et al., *SAV1 promotes Hippo kinase activation through antagonizing the PP2A phosphatase STRIPAK.* eLife, 2017. **6**: p. e30278.
16. Pan, D., *The Hippo Signaling Pathway in Development and Cancer.* Developmental cell, 2010. **19**(4): p. 491-505.

17. Elbediwy, A., Z.I. Vincent-Mistiaen, and B.J. Thompson, *YAP and TAZ in epithelial stem cells: A sensor for cell polarity, mechanical forces and tissue damage.* Bioessays, 2016. **38**(7): p. 644-653.
18. Dumbauld, D.W., et al., *How vinculin regulates force transmission.* Proceedings of the National Academy of Sciences, 2013. **110**(24): p. 9788.
19. Nardone, G., et al., *YAP regulates cell mechanics by controlling focal adhesion assembly.* Nature Communications, 2017. **8**: p. 15321.
20. Aragona, M., et al., *A Mechanical Checkpoint Controls Multicellular Growth through YAP/TAZ Regulation by Actin-Processing Factors.* Cell, 2013. **154**(5): p. 1047-1059.
21. Zhao, B., et al., *Cell detachment activates the Hippo pathway via cytoskeleton reorganization to induce anoikis.* Genes & Development, 2012. **26**(1): p. 54-68.
22. Padmanabhan, A., H.T. Ong, and R. Zaidel-Bar, *Non-junctional E-Cadherin Clusters Regulate the Actomyosin Cortex in the C. elegans Zygote.* Current Biology, 2017. **27**(1): p. 103-112.
23. Rauskolb, C., et al., *Cytoskeletal Tension inhibits Hippo signaling through an Ajuba-Warts complex.* Cell, 2014. **158**(1): p. 143-156.
24. Su, T., et al., *Kibra and Merlin Activate the Hippo Pathway Spatially Distinct from and Independent of Expanded.* Developmental cell, 2017. **40**(5): p. 478-490.e3.
25. Szymaniak, A.D., et al., *Crumbs3-Mediated Polarity Directs Airway Epithelial Cell Fate through the Hippo Pathway Effector Yap.* Developmental cell, 2015. **34**(3): p. 283-296.
26. Zhang, N., et al., *The Merlin/NF2 tumor suppressor functions through the YAP oncoprotein to regulate tissue homeostasis in mammals.* Developmental cell, 2010. **19**(1): p. 27-38.
27. Elbediwy, A. and B.J. Thompson, *Evolution of mechanotransduction via YAP/TAZ in animal epithelia.* Curr Opin Cell Biol, 2018. **51**: p. 117-123.
28. Sun, S., B.V.V.G. Reddy, and K.D. Irvine, *Localization of Hippo signalling complexes and Warts activation in vivo.* Nature Communications, 2015. **6**: p. 8402.
29. Fletcher, G.C., et al., *The Spectrin cytoskeleton regulates the Hippo signalling pathway.* The EMBO journal, 2015. **34**(7): p. 940-954.
30. Sun, S. and K.D. Irvine, *Cellular Organization and Cytoskeletal Regulation of the Hippo Signaling Network.* Trends in cell biology, 2016. **26**(9): p. 694-704.
31. Fletcher, G.C., et al., *Mechanical strain regulates the Hippo pathway in Drosophila.* Development (Cambridge, England). **145**(5): p. dev159467.
32. Mo, J.-S., *The role of extracellular biophysical cues in modulating the Hippo-YAP pathway.* BMB reports, 2017. **50**(2): p. 71-78.
33. Yu, F.-X., et al., *Regulation of the Hippo-YAP pathway by G-protein-coupled receptor signaling.* Cell, 2012. **150**(4): p. 780-791.
34. Yu, F.-X. and K.-L. Guan, *The Hippo pathway: regulators and regulations.* Genes & development, 2013. **27**(4): p. 355-371.
35. Mihaylova, M.M. and R.J. Shaw, *The AMPK signalling pathway coordinates cell growth, autophagy and metabolism.* Nature cell biology, 2011. **13**(9): p. 1016-1023.

36. Loewith, R. and M.N. Hall, *Target of rapamycin (TOR) in nutrient signaling and growth control.* Genetics, 2011. **189**(4): p. 1177-1201.
37. Mo, J.-S., et al., *Cellular energy stress induces AMPK-mediated regulation of YAP and the Hippo pathway.* Nature cell biology, 2015. **17**(4): p. 500-510.
38. Parker, J. and G. Struhl, *Scaling the Drosophila Wing: TOR-Dependent Target Gene Access by the Hippo Pathway Transducer Yorkie.* PLoS biology, 2015. **13**(10): p. e1002274-e1002274.
39. Marinari, E., et al., *Live-cell delamination counterbalances epithelial growth to limit tissue overcrowding.* Nature, 2012. **484**: p. 542.
40. Levayer, R., C. Dupont, and E. Moreno, *Tissue Crowding Induces Caspase-Dependent Competition for Space.* Current Biology, 2016. **26**(5): p. 670-677.
41. Costa, M., et al., *The bristle patterning genes hairy and extramacrochaetae regulate the development of structures required for flight in Diptera.* Developmental biology, 2014. **388**(2): p. 205-215.
42. *A new model for single-cell delamination.* Development, 2017. **144**(12): p. e1204.
43. Parisi, F. and M. Vidal, *Epithelial delamination and migration: lessons from Drosophila.* Cell adhesion & migration, 2011. **5**(4): p. 366-372.
44. Toyama, Y., et al., *Apoptotic force and tissue dynamics during Drosophila embryogenesis.* Science (New York, N.Y.), 2008. **321**(5896): p. 1683-1686.
45. Wagstaff, L., et al., *Mechanical cell competition kills cells via induction of lethal p53 levels.* Nature Communications, 2016. **7**: p. 11373.
46. Coste, B., et al., *Piezo1 and Piezo2 are essential components of distinct mechanically activated cation channels.* Science (New York, N.Y.), 2010. **330**(6000): p. 55-60.
47. Pathak, M.M., et al., *Stretch-activated ion channel Piezo1 directs lineage choice in human neural stem cells.* Proceedings of the National Academy of Sciences of the United States of America, 2014. **111**(45): p. 16148-16153.
48. Gudipaty, S.A., et al., *Mechanical stretch triggers rapid epithelial cell division through Piezo1.* Nature, 2017. **543**(7643): p. 118-121.
49. He, L., et al., *Mechanical regulation of stem-cell differentiation by the stretch-activated Piezo channel.* Nature, 2018. **555**(7694): p. 103-106.
50. Lifshitz, V. and D. Frenkel, *Chapter 225 - TGF-β*, in *Handbook of Biologically Active Peptides (Second Edition)*, A.J. Kastin, Editor. 2013, Academic Press: Boston. p. 1647-1653.
51. Raftery, L.A. and D.J. Sutherland, *TGF-β Family Signal Transduction in Drosophila Development: From Mad to Smads.* Developmental Biology, 1999. **210**(2): p. 251-268.
52. Nallet-Staub, F., et al., *Cell Density Sensing Alters TGF-β Signaling in a Cell-Type-Specific Manner, Independent from Hippo Pathway Activation.* Developmental cell, 2015. **32**(5): p. 640-651.
53. Horbelt, D., A. Denkis, and P. Knaus, *A portrait of Transforming Growth Factor β superfamily signalling: Background matters.* The International Journal of Biochemistry & Cell Biology, 2012. **44**(3): p. 469-474.
54. Varelas, X., et al., *The Crumbs Complex Couples Cell Density Sensing to Hippo-Dependent Control of the TGF-β-SMAD Pathway.* Developmental Cell, 2010. **19**(6): p. 831-844.

55. Silginer, M., et al., *The aryl hydrocarbon receptor links integrin signaling to the TGF-β pathway.* Oncogene, 2015. **35**: p. 3260.
56. Roth, P., et al., *Integrin control of the transforming growth factor-β pathway in glioblastoma.* Brain, 2013. **136**(2): p. 564-576.
57. Galgoczi, E., et al., *Cell density-dependent stimulation of PAI-1 and hyaluronan synthesis by TGF-β in orbital fibroblasts.* The Journal Of Endocrinology, 2016. **229**(2): p. 187-196.
58. Stanley, A.J., et al., *Effect of cell density on the expression of adhesion molecules and modulation by cytokines.* Cytometry, 1995. **21**(4): p. 338-343.
59. Arbouzova, N.I. and M.P. Zeidler, *JAK/STAT signalling in Drosophila: insights into conserved regulatory and cellular functions.* Development (Cambridge, England), 2006. **133**(14): p. 2605-2616.
60. Zoranovic, T., L. Grmai, and E.A. Bach, *Regulation of proliferation, cell competition, and cellular growth by the Drosophila JAK-STAT pathway.* JAK-STAT, 2013. **2**(3): p. e25408.
61. Vidal, O.M., et al., *Negative regulation of Drosophila JAK–STAT signalling by endocytic trafficking.* Journal of Cell Science, 2010. **123**(20): p. 3457-3466.
62. Mukherjee, T., J.C.-G. Hombría, and M.P. Zeidler, *Opposing roles for Drosophila JAK/STAT signalling during cellular proliferation.* Oncogene, 2005. **24**: p. 2503.
63. Borensztejn, A., A. Mascaro, and K.A. Wharton, *JAK/STAT signaling prevents excessive apoptosis to ensure maintenance of the interfollicular stalk critical for Drosophila oogenesis.* Developmental Biology, 2018. **438**(1): p. 1-9.
64. Lin, T.-H., et al., *The Hippo Pathway Controls Border Cell Migration Through Distinct Mechanisms in Outer Border Cells and Polar Cells of the Drosophila Ovary.* Genetics, 2014. **198**(3): p. 1087-1099.
65. Kreis, S., et al., *Cell Density–Dependent Increase of Constitutive Signal Transducers and Activators of Transcription 3 Activity in Melanoma Cells Is Mediated by Janus Kinases.* Molecular Cancer Research, 2007. **5**(12): p. 1331.
66. Anagnostopoulou, A., et al., *Differential effects of Stat3 inhibition in sparse vs confluent normal and breast cancer cells.* Cancer Letters, 2006. **242**(1): p. 120-132.
67. Torres, A.Y., et al., *JAK/STAT signaling is necessary for cell monosis prior to epithelial cell apoptotic extrusion.* Cell Death &Amp; Disease, 2017. **8**: p. e2814.
68. Richardson, H.E. and M. Portela, *Tissue growth and tumorigenesis in Drosophila: cell polarity and the Hippo pathway.* Curr Opin Cell Biol, 2017. **48**: p. 1-9.
69. Stramer, B. and R. Mayor, *Mechanisms and in vivo functions of contact inhibition of locomotion.* Nat Rev Mol Cell Biol, 2016.
70. Schulze, A. and A.L. Harris, *How cancer metabolism is tuned for proliferation and vulnerable to disruption.* Nature, 2012. **491**(7424): p. 364-73.
71. Cooper, J.P. and R.J. Youle, *Balancing cell growth and death.* Curr Opin Cell Biol, 2012. **24**(6): p. 802-3.
72. Thompson, B.J., *Developmental control of cell growth and division in Drosophila.* Curr Opin Cell Biol, 2010. **22**(6): p. 788-94.
73. Sharif, G.M. and A. Wellstein, *Cell density regulates cancer metastasis via the Hippo pathway.* Future Oncol, 2015. **11**(24): p. 3253-60.

74. Zeng, Q. and W. Hong, *The emerging role of the hippo pathway in cell contact inhibition, organ size control, and cancer development in mammals.* Cancer Cell, 2008. **13**(3): p. 188-92.
75. Hayes, C.S., et al., *Mechanisms and biological roles of contact-dependent growth inhibition systems.* Cold Spring Harb Perspect Med, 2014. **4**(2).
76. Li, M., V.E. Belozerov, and H.N. Cai, *Analysis of chromatin boundary activity in Drosophila cells.* BMC Mol Biol, 2008. **9**: p. 109.
77. Small, S., A. Blair, and M. Levine, *Regulation of even-skipped stripe 2 in the Drosophila embryo.* Embo J, 1992. **11**(11): p. 4047-57.
78. Bunch, T.A., Y. Grinblat, and L.S. Goldstein, *Characterization and use of the Drosophila metallothionein promoter in cultured Drosophila melanogaster cells.* Nucleic Acids Res, 1988. **16**(3): p. 1043-61.
79. Cai, H.N. and M. Levine, *The gypsy insulator can function as a promoter-specific silencer in the Drosophila embryo.* EMBO J, 1997. **16**(7): p. 1732-41.
80. Cai, H.N., et al., *Genomic context modulates insulator activity through promoter competition.* Development, 2001. **128**(21): p. 4339-47.
81. Barolo, S., B. Castro, and J.W. Posakony, *New Drosophila transgenic reporters: insulated P-element vectors expressing fast-maturing RFP.* Biotechniques, 2004. **36**(3): p. 436-40, 442.
82. Bevis, B.J. and B.S. Glick, *Rapidly maturing variants of the Discosoma red fluorescent protein (DsRed).* Nat Biotechnol, 2002. **20**(1): p. 83-7.
83. Jacobson, K.B., et al., *Toxic and biochemical effects of divalent metal ions in Drosophila: correlation to effects in mice and to chemical softness parameters.* Sci Total Environ, 1983. **28**: p. 355-66.
84. Lastowski-Perry, D., E. Otto, and G. Maroni, *Nucleotide sequence and expression of a Drosophila metallothionein.* J Biol Chem, 1985. **260**(3): p. 1527-30.
85. Segal, D., L. Cherbas, and P. Cherbas, *Genetic transformation of Drosophila cells in culture by P element-mediated transposition.* Somat Cell Mol Genet, 1996. **22**(2): p. 159-65.
86. Rubin, G.M. and A.C. Spradling, *Genetic transformation of Drosophila with transposable element vectors.* Science, 1982. **218**(4570): p. 348-53.
87. Gunther, V., U. Lindert, and W. Schaffner, *The taste of heavy metals: gene regulation by MTF-1.* Biochim Biophys Acta, 2012. **1823**(9): p. 1416-25.
88. Ohtsuki, S. and M. Levine, *GAGA mediates the enhancer blocking activity of the eve promoter in the Drosophila embryo.* Genes Dev, 1998. **12**(21): p. 3325-3330.
89. Steller, H. and V. Pirrotta, *A transposable P vector that confers selectable G418 resistance to Drosophila larvae.* EMBO J, 1985. **4**(1): p. 167-71.
90. Pirrotta, V., *Vectors for P-mediated transformation in Drosophila.* Biotechnology, 1988. **10**: p. 437-56.
91. Steller, H. and V. Pirrotta, *P transposons controlled by the heat shock promoter.* Mol Cell Biol, 1986. **6**(5): p. 1640-9.
92. Cai, H.N., D.N. Arnosti, and M. Levine, *Long-range repression in the Drosophila embryo.* Proc Natl Acad Sci U S A, 1996. **93**(18): p. 9309-14.
93. Jiang, J., et al., *Conversion of a dorsal-dependent silencer into an enhancer: evidence for dorsal corepressors.* Embo J, 1993. **12**(8): p. 3201-9.

94. Jiang, J., et al., *The dorsal morphogen gradient regulates the mesoderm determinant twist in early Drosophila embryos.* Genes Dev, 1991. **5**(10): p. 1881-91.
95. Pedersen, M.O., et al., *Metallothionein-I + II and receptor megalin are altered in relation to oxidative stress in cerebral lymphomas.* Leuk Lymphoma, 2010. **51**(2): p. 314-28.
96. Murphy, B.J., et al., *Metallothionein induction by hypoxia involves cooperative interactions between metal-responsive transcription factor-1 and hypoxia-inducible transcription factor-1alpha.* Mol Cancer Res, 2008. **6**(3): p. 483-90.
97. Corbin, V. and T. Maniatis, *The role of specific enhancer-promoter interactions in the Drosophila Adh promoter switch.* Genes Dev, 1989. **3**(12B): p. 2191-20.
98. Tokuda, Y., et al., *The levels and kinetics of oxygen tension detectable at the surface of human dermal fibroblast cultures.* J Cell Physiol, 2000. **182**(3): p. 414-20.
99. Pettersen, E.O., et al., *Pericellular oxygen depletion during ordinary tissue culturing, measured with oxygen microsensors.* Cell Prolif, 2005. **38**(4): p. 257-67.
100. Sheta, E.A., et al., *Cell density mediated pericellular hypoxia leads to induction of HIF-1alpha via nitric oxide and Ras/MAP kinase mediated signaling pathways.* Oncogene, 2001. **20**(52): p. 7624-34.
101. Place, T.L., F.E. Domann, and A.J. Case, *Limitations of oxygen delivery to cells in culture: An underappreciated problem in basic and translational research.* Free Radic Biol Med, 2017. **113**: p. 311-322.
102. Murphy, B.J., et al., *The metal-responsive transcription factor-1 contributes to HIF-1 activation during hypoxic stress.* Biochem Biophys Res Commun, 2005. **337**(3): p. 860-7.
103. Li, L., et al., *Desferrioxamine regulates HIF-1 alpha expression in neonatal rat brain after hypoxia-ischemia.* Am J Transl Res, 2014. **6**(4): p. 377-83.
104. Bala, K. and N.K. Gohil, *Interaction of glycated protein and DFO mimicked hypoxia in cellular responses of HUVECs.* Mol Biosyst, 2012. **8**(10): p. 2657-63.
105. Romero, N.M., et al., *Regulation of the Drosophila hypoxia-inducible factor alpha Sima by CRM1-dependent nuclear export.* Mol Cell Biol, 2008. **28**(10): p. 3410-23.
106. Lee, S.J., R. Feldman, and P.H. O'Farrell, *An RNA interference screen identifies a novel regulator of target of rapamycin that mediates hypoxia suppression of translation in Drosophila S2 cells.* Mol Biol Cell, 2008. **19**(10): p. 4051-61.
107. Kraggerud, S.M., J.A. Sandvik, and E.O. Pettersen, *Regulation of protein synthesis in human cells exposed to extreme hypoxia.* Anticancer Res, 1995. **15**(3): p. 683-6.
108. Liu, L., et al., *Hypoxia-induced energy stress regulates mRNA translation and cell growth.* Mol Cell, 2006. **21**(4): p. 521-31.
109. Stein, I., et al., *Translation of vascular endothelial growth factor mRNA by internal ribosome entry: implications for translation under hypoxia.* Mol Cell Biol, 1998. **18**(6): p. 3112-9.

110. Murphy, B.J., et al., *Activation of metallothionein gene expression by hypoxia involves metal response elements and metal transcription factor-1.* Cancer Res, 1999. **59**(6): p. 1315-22.
111. Hinds, P.W., et al., *Regulation of retinoblastoma protein functions by ectopic expression of human cyclins.* Cell, 1992. **70**(6): p. 993-1006.
112. Keyomarsi, K. and T.W. Herliczek, *The role of cyclin E in cell proliferation, development and cancer.* Prog Cell Cycle Res, 1997. **3**: p. 171-91.
113. Kondo, T., T. Yokokura, and S. Nagata, *Activation of distinct caspase-like proteases by Fas and reaper in Drosophila cells.* Proc Natl Acad Sci U S A, 1997. **94**(22): p. 11951-6.
114. White, K., E. Tahaoglu, and H. Steller, *Cell killing by the Drosophila gene reaper.* Science, 1996. **271**(5250): p. 805-7.
115. Song, Z., et al., *Biochemical and genetic interactions between Drosophila caspases and the proapoptotic genes rpr, hid, and grim.* Mol Cell Biol, 2000. **20**(8): p. 2907-14.
116. Hamaratoglu, F., et al., *The tumour-suppressor genes NF2/Merlin and Expanded act through Hippo signalling to regulate cell proliferation and apoptosis.* Nat Cell Biol, 2006. **8**(1): p. 27-36.
117. Yin, F., et al., *Spatial organization of Hippo signaling at the plasma membrane mediated by the tumor suppressor Merlin/NF2.* Cell, 2013. **154**(6): p. 1342-55.
118. Justice, R.W., et al., *The Drosophila tumor suppressor gene warts encodes a homolog of human myotonic dystrophy kinase and is required for the control of cell shape and proliferation.* Genes & Development, 1995. **9**(5): p. 534-546.
119. Tsukamoto, H., et al., *Alpha-smooth muscle actin expression in tumor and stromal cells of benign and malignant human pigment cell tumors.* J Invest Dermatol, 1992. **98**(1): p. 116-20.
120. Kobayashi, H., et al., *Expression of alpha-smooth muscle actin in benign or malignant ovarian tumors.* Gynecol Oncol, 1993. **48**(3): p. 308-13.
121. Eder, D., C. Aegerter, and K. Basler, *Forces controlling organ growth and size.* Mech Dev, 2017. **144**(Pt A): p. 53-61.
122. Lemke, S.B. and F. Schnorrer, *Mechanical forces during muscle development.* Mech Dev, 2017. **144**(Pt A): p. 92-101.
123. Kourtidis, A., et al., *A central role for cadherin signaling in cancer.* Exp Cell Res, 2017. **358**(1): p. 78-85.
124. Talele, N.P., et al., *Expression of alpha-Smooth Muscle Actin Determines the Fate of Mesenchymal Stromal Cells.* Stem Cell Reports, 2015. **4**(6): p. 1016-30.
125. Hinz, B., et al., *Alpha-smooth muscle actin expression upregulates fibroblast contractile activity.* Mol Biol Cell, 2001. **12**(9): p. 2730-41.
126. Goffin, J.M., et al., *Focal adhesion size controls tension-dependent recruitment of alpha-smooth muscle actin to stress fibers.* J Cell Biol, 2006. **172**(2): p. 259-68.
127. Schmitt-Ney, M. and J.F. Habener, *Cell-density-dependent regulation of actin gene expression due to changes in actin treadmilling.* Exp Cell Res, 2004. **295**(1): p. 236-44.
128. Campbell, H.D., et al., *Fliih, a gelsolin-related cytoskeletal regulator essential for early mammalian embryonic development.* Mol Cell Biol, 2002. **22**(10): p. 3518-26.

129. Stella, M.C., et al., *Identification of secreted and cytosolic gelsolin in Drosophila.* J Cell Biol, 1994. **125**(3): p. 607-16.
130. Campbell, H.D., et al., *The Drosophila melanogaster flightless-I gene involved in gastrulation and muscle degeneration encodes gelsolin-like and leucine-rich repeat domains and is conserved in Caenorhabditis elegans and humans.* Proc Natl Acad Sci U S A, 1993. **90**(23): p. 11386-90.
131. Bearer, E.L., *Direct observation of actin filament severing by gelsolin and binding by gCap39 and CapZ.* J Cell Biol, 1991. **115**(6): p. 1629-38.
132. Ziller, A. and L. Fraissinet-Tachet, *Metallothionein diversity and distribution in the tree of life: a multifunctional protein.* Metallomics, 2018.
133. Palmiter, R.D., *The elusive function of metallothioneins.* Proc Natl Acad Sci U S A, 1998. **95**(15): p. 8428-30.
134. Penkowa, M., *Metallothioneins are multipurpose neuroprotectants during brain pathology.* FEBS J, 2006. **273**(9): p. 1857-70.
135. Sogawa, C.A., et al., *Localization, regulation, and function of metallothionein-III/growth inhibitory factor in the brain.* Acta Med Okayama, 2001. **55**(1): p. 1-9.
136. Howells, C., A.K. West, and R.S. Chung, *Neuronal growth-inhibitory factor (metallothionein-3): evaluation of the biological function of growth-inhibitory factor in the injured and neurodegenerative brain.* FEBS J, 2010. **277**(14): p. 2931-9.
137. Schito, L. and S. Rey, *Cell-Autonomous Metabolic Reprogramming in Hypoxia.* Trends Cell Biol, 2018. **28**(2): p. 128-142.
138. Gonzalez, F.J., C. Xie, and C. Jiang, *The role of hypoxia-inducible factors in metabolic diseases.* Nat Rev Endocrinol, 2018.
139. Choudhry, H. and A.L. Harris, *Advances in Hypoxia-Inducible Factor Biology.* Cell Metab, 2018. **27**(2): p. 281-298.
140. Muz, B., et al., *The role of hypoxia in cancer progression, angiogenesis, metastasis, and resistance to therapy.* Hypoxia (Auckl), 2015. **3**: p. 83-92.
141. Arsham, A.M., J.J. Howell, and M.C. Simon, *A novel hypoxia-inducible factor-independent hypoxic response regulating mammalian target of rapamycin and its targets.* J Biol Chem, 2003. **278**(32): p. 29655-60.
142. Heacock, C.S. and R.M. Sutherland, *Enhanced synthesis of stress proteins caused by hypoxia and relation to altered cell growth and metabolism.* Br J Cancer, 1990. **62**(2): p. 217-25.
143. Billmann, M. and M. Boutros, *Methods for High-Throughput RNAi Screening in Drosophila Cells.* Methods Mol Biol. , 2016(1478).
144. Lipinski, S., et al., *RNAi screening identifies mediators of NOD2 signaling: Implications for spatial specificity of MDP recognition.* Proceedings of the National Academy of Sciences of the United States of America, 2012. **109**(52): p. 21426-21431.
145. Heltemes-Harris, L.M., et al., *Sleeping Beauty transposon screen identifies signaling modules that cooperate with STAT5 activation to induce B-cell acute lymphoblastic leukemia.* Oncogene, 2016. **35**(26): p. 3454-3464.
146. Burnette, M., et al., *An inverse small molecule screen to design a chemically defined medium supporting long-term growth of Drosophila cell lines.* Molecular Biosystems, 2014. **10**(10): p. 2713-2723.

147. Pawar, V., et al., *RNAi Screening of Drosophila (Sophophora) melanogaster S2 Cells for Ricin Sensitivity and Resistance.* Journal of Biomolecular Screening, 2011. **16**(4): p. 436-442.
148. Palmiter, R.D. and R.L. Brinster, *Germ-line transformation of mice.* Annu Rev Genet, 1986. **20**: p. 465-99.
149. Kalfayan, L., B. Wakimoto, and A. Spradling, *Analysis of transcriptional regulation of the s38 chorion gene of Drosophila by P element-mediated transformation.* J Embryol Exp Morphol, 1984. **83 Suppl**: p. 137-46.
150. Stanojevic, D., S. Small, and M. Levine, *Regulation of a segmentation stripe by overlapping activators and repressors in the Drosophila embryo.* Science, 1991. **254**(5036): p. 1385-7.
151. Sansores-Garcia, L., et al., *Mask is required for the activity of the Hippo pathway effector Yki/YAP.* Current biology : CB, 2013. **23**(3): p. 229-235.
152. Reddy, B.V.V.G. and K.D. Irvine, *Regulation of Drosophila glial cell proliferation by Merlin-Hippo signaling.* Development (Cambridge, England), 2011. **138**(23): p. 5201-5212.
153. Moutinho-Pereira, S., I. Matos, and H. Maiato, *Drosophila S2 Cells as a Model System to Investigate Mitotic Spindle Dynamics, Architecture, and Function*. 2010, ACADEMIC PRESS: Great Britain. p. 243.
154. Dowling, P. and M. Clynes, *Conditioned media from cell lines: A complementary model to clinical specimens for the discovery of disease-specific biomarkers.* PROTEOMICS, 2010. **11**(4): p. 794-804.
155. Kadekar, D., et al., *Conditioned Medium from Placental Mesenchymal Stem Cells Reduces Oxidative Stress during the Cryopreservation of Ex Vivo Expanded Umbilical Cord Blood Cells.* PLOS ONE, 2016. **11**(10): p. e0165466.
156. Ribeiro, C.A., et al., *The secretome of bone marrow mesenchymal stem cells-conditioned media varies with time and drives a distinct effect on mature neurons and glial cells (primary cultures).* Journal of Tissue Engineering and Regenerative Medicine, 2011. **5**(8): p. 668-672.
157. Sohn, S.J., et al., *Anti-aging Properties of Conditioned Media of Epidermal Progenitor Cells Derived from Mesenchymal Stem Cells.* Dermatology and therapy, 2018. **8**(2): p. 229-244.
158. Ribeiro, S.A., M.V. D'Ambrosio, and R.D. Vale, *Induction of focal adhesions and motility in Drosophila S2 cells.* Molecular Biology of the Cell, 2014. **25**(24): p. 3861-3869.
159. Rago, A.P., et al., *Miniaturization of an Anoikis assay using non-adhesive micromolded hydrogels.* Cytotechnology, 2008. **56**(2): p. 81-90.
160. Tanaka, E.M., *The Molecular and Cellular Choreography of Appendage Regeneration.* Cell, 2016. **165**(7): p. 1598-1608.
161. Rogers, S.L., et al., *Molecular requirements for actin-based lamella formation in Drosophila S2 cells.* The Journal of Cell Biology, 2003. **162**(6): p. 1079-1088.
162. Bodeen, W.J., et al., *A fixation method to preserve cultured cell cytonemes facilitates mechanistic interrogation of morphogen transport.* Development (Cambridge, England), 2017. **144**(19): p. 3612-3624.